FURTHER APPLICATIONS OF A GLUTAMATE OXIDASE REACTOR FOR THE DETERMINATION OF THE NEUROTOXIN β-ODAP IN A FLOW INJECTION SYSTEM

A Thesis
Presented to
The School of Graduate Studies
Addis Ababa University

In Partial Fulfilment of
The Requirement for the Degree
of Master of Science in Chemistry

BY

Abebaw Belay

June, 1995

ADDIS ABABA UNIVERSITY

SCHOOL OF GRADUATE STUDIES

FURTHER APPLICATIONS OF A GLUTAMATE OXIDASE REACTOR FOR THE DETERMINATION OF THE NEUROTOXIN β-ODAP IN A FLOW INJECTION SYSTEM

BY

Abebaw Belay

Chemistry Department

Science Faculty

Approved by:

Dr. Ghirma Moges
Advisor

Dr. Theodros Solomon
Advisor

Prof. Lo Gorton
Examiner

Dr. B.S. Chandravanshi
Examiner

Dr. B. Hundhammer
Examiner

TABLE OF CONTENTS

ACKNOWLEDGMENTS

I want to express my sincere gratitude to my research advisors Dr Ghirma Moges and Dr Theodros Solomon for identifying the topic for my research work. It is with great pleasure that I express my heartfelt gratitude and sincere thanks to Dr Ghirma Moges for his consistent guidance and warm welcome to open discussion of any degree in every phase of the research.

I am very grateful to Professor Gillis Johansson (Department of Analytical Chemistry, University of Lund, Sweden) for sending me some reagents and accessaries for the flow injection system .

I wish to express my gratitude to Ato Amare Gessesse (Biology Department, AAU) for allowing me to use some of the laboratory equipment and fruitful discussion. Dr H. Kusakabe (Yamasa Corporation, Japan) is acknowledged for donation of glutamate oxidase. Dr Berhanu Abegaz and his research group, Dr Gizachew Alemayehu and Ato Yirgalem Yigzaw, for supplying ODAP and grass pea samples. Ato Yirgalem synthesized and independently assayed ODAP in grass pea samples using the OPT method. My thanks also goes to Ato Merid Tessema for the interest that he showed to the work.

I owe a lot to my parents and friends for the understanding and cooperation they have shown to me during the period of my study.

I am grateful to the staff members of the Chemistry Department and would like also to acknowledge the Department of Chemistry, AAU, for giving me the opportunity to participate in the graduate programme.

I acknowledge the financial support from DEUTSCHER AKADEMISCHER AUSTAUSCHDIENST (DAAD) during the period of my study. Finally, material support for the project from the Swedish Agency for Research Co-operation with developing countries (SAREC) is highly acknowledeged.

LIST OF FIGURES

LIST OF TABLES

ABSTRACT

FURTHER APPLICATIONS OF A GLUTAMATE OXIDASE REACTOR FOR THE DETERMINATION OF THE NEUROTOXIN β-ODAP IN A FLOW INJECTION SYSTEM

By

Abebaw Belay

Research advisors: Dr Ghirma Moges and Dr Theodros Solomon

A flow injection system involving immobilized GlOD reactor was employed to study the kinetics of the isomerization of β-ODAP to α-ODAP. The amino acid was oxidized by dissolved oxygen to produce hydrogen peroxide which subsequently reacted with Trinder chromogenic reagent (catalyzed by horseradish peroxidase in solution, HRP) to form red-coloured quinone imine dye for spectrophotometric detection at 512 nm. Injections of 20 μl β-ODAP standards resulted in a linear range of 10 - 300 μM. Thermal treatment (at 80 °C) of β-ODAP standards and grass pea extracts reduced the FI response to 62 - 63% of that before heating, because of the isomerization of the β-isomer to the non-toxic α-isomer. This reconfirms the reported selectivity of GlOD to the toxin. The experimental convenience of the β-selective flow system has been exploited to study the effects of the neurotoxin concentration and temperature on the rates of β-α conversion. The results of these studies showed that the isomerization of the toxin to the nontoxic isomer followed zero order kinetics with an initial apparent rate constant equal to 15.26 μM/min. The equilibrium time varied linearly with the initial concentration of β-ODAP. Values for the initial apparent rate constant of isomerization (at pH 7) were 3.56 μM/min, 6.28 μM/min, 15.26 μM/min and 30.89 μM/min at 60, 70, 80 and 90°C , respectively. Isomerization at pH 2 proceeded at a faster rate (24.5 μM/min) than at pH 7.

The complete flow injection set-up for the determination of β-ODAP in grass pea samples consisted of two packed-bed enzyme reactors in series, namely a mixture of GlOD (25 μl) and catalase (25 μl), and GlOD (250 μl). The major interference from glutamate was destroyed by its quantitative oxidation in the pre-reactor. The product,

hydrogen peroxide, was destroyed in the first reactor which contained GIOD and catalase. Most of the β-ODAP was oxidized in the big (250 μl) reactor, because only a few percent of this compound is destroyed in the first reactor. The β-ODAP concentrations of five grass pea samples (0.599 - 0.749%) were determined from flow injection peaks of filtered extracts in phosphate buffer (pH 7). These results were found to be in good agreement with the values obtained using the OPT method.

Chapter 1

1.0 INTRODUCTION

The study of toxins associated with plant materials whose consumption either by humans or by domestic animals result in certain types of diseases, deformities or characteristic pharmacological effects, have been receiving considerable attention in recent years. Lathyrism is one case of such diseases of dietary origin, in which investigations of the problem in different aspects have been made in the past few years.

The term Lathyrism was introduced by Cantoni in 1873 pointing to symptoms following the ingestion of *lathyrus* species, the chuckling pea.

Two toxic syndromes have generally been associated with the ingestion of *lathyrus* seeds. Osteolathyrism or odoratism refers to the effect observed in rats and other animals following the ingestion of the seeds of *L.odoratus, L.hirsutus* and *L.pusillus*. The pathological changes are mainly in the skeleton and connective tissues. β-Amino-propionitrile seems to be the responsible agent [1]. Lathyrism or neurolathyrism describes symptoms observed in man due to the ingestion of seeds of L.*sativus*, although seeds of *L.cicera* and *L.clymenum* have also been implicated [2].

1.1 NEUROLATHYRISM

The seeds of *lathyrus sativus*, LS, (grass pea, also known as guaya in Amharic, Khesari in India and Bangladesh), a legume widely cultivated in Ethiopia, India, Bangladesh, and Nepal, provide a nourishing diet of high quality protein and carbohydrates. The protein content of this edible seed is 26-30%. The plant is still widely cultivated in the cited countries mainly due to three reasons: (1) It is the cheapest leguminous pulse available to the poor man (2) people are accustomed to its consumption, and (3) it is a hardy crop requiring very little agricultural attention and is considered as life-saving at times of drought and famine. The legume is widely cultivated in areas where farmers are dependent on rain-fed agriculture and it occupies a significant proportion of the pulses produced in these areas (e.g., Ethiopia 7.5%, Bangladesh 34%, and India in millions of hectares) [3]. It has, therefore, been an important alternative source of protein for human consumption and fodder for livestock.

Neurolathyrism is characterized by such symptoms as muscular rigidity, weakness and paralysis of the leg muscles, convulsions, head retraction, stiffening of neck and death in extreme cases [4]. Cranial nerve involvement, sensory-motor neuropathies and urinary bladder disturbances are rare additional findings in the chronic stage [4]. The disease reaches epidemic proportions in times of famine caused by flood and drought [5]. Relatively recently, outbreaks of lathyrism occurred in Ethiopia and Bangladesh [5]. In Ethiopia, the disease occurs in the northern and central parts of the country with recent outbreaks reported from the Lake Tana basin of the north-west Administrative Region of Gondar.

In humans, the use of LS one-third to one-half of the diet for two or three months was considered enough to cause the disease, although not all persons eating he diet seemed to be affected; in families only certain members were attacked. Males were said to be more susceptible than females [6-8].

1.1.1 HISTORY

Lathyrism is a disease of great antiquity. The toxicity of LS seeds has been known in the western and eastern world since historical times. The ancient old Hindu medical text, Bhavaprakasa mentions the fact that "the triputa pulse causes a man to become lame and crippled and it irritates the nerves" [4]. In the western world Hippocrates (460-377 BC) gave the first account of it in his book of Epidemics: "At Ainos all men and women who ate peas continuously became impotent in the legs and that state persisted" [1, 4]. In 1671, Duke George of Wurttemberg was the first to prohibit the consumption of bread baked with this pea, followed by prohibitions in India and other countries [1, 4]. Nevertheless, even now, the chuckling pea is part of the daily food intake among the poor in some parts of India, Ethiopia and Bangladesh.

1.1.2 THE TOXIC PRINCIPLE

The toxin responsible for human lathyrism, identified 30 years ago by two independent research groups in India [9, 10], is the non-essential amino acid: β-N-Oxalyl-L-α,β-diaminopropionic acid, β-ODAP, (or its synonym β-N-Oxalylamino-L-alanine, BOAA). β-ODAP has been detected in seeds of 21 *lathyrus* species, 17 *Acacia* species and 13 *crotalaria* species [11]. The neurotoxicity of β-ODAP has recently been confirmed [12]. The chemical structure of the toxic compound is

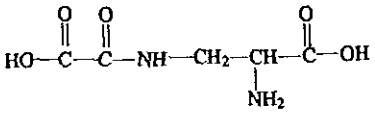

β-ODAP is found to be a powerful convulsant [9] and is neuroexcitatory to central nervous system neurones, acting at the quisqulate and kainate receptors [13]. In the plant the amino acid exists as two isomeric forms; alpha and beta. The α-isomer is present to the extent of approximately 5% in the seed and is found to be non- or low-toxic [14]. Study on the biosynthesis of the neurolathyrogen ODAP showed that an unstable heterocyclic amino acid β-(isoxazolin-5-on-2-yl)-L-alanine (BIA) is the precursor for the in *vivo* biosynthesis of ODAP [15].

As early as 1966, Bell and O'Donovan reported that in ethanolic solution β-ODAP slowly equilibrates with the α-isomer and the interconvertion is facilitated when heated [16]. The non-toxicity of the α-isomer and the observation that the β-isomer which is present in the seed may be isomerized to the non-toxic form paves a way to explore various processing and cooking methods as a means of thermal detoxification of the legume.

Since seeds of LS have high nutritional value and are able to withstand drought and other extreme conditions, it is, therefore, important that means be devised to make this legume free from the toxic component so that it can serve as food crop in regions of the world subjected to drought.

1.1.3 ANALYTICAL METHODS FOR THE DETERMINATION OF β-ODAP

The problem of lathyrism has been well addressed by workers in agronomy, nutrition, neurology, pharmacology, and chemistry [3,17]. Intensive research for developing low toxin or zero toxin varieties of LS seeds is going on in several institutes [3,17]. The most obvious option to achieve this goal entails plant breeding and genetic programs [3, 17]. Detoxification before ingestion is the other alternative to combat lathyrism. This involves processing a large number of samples, requiring fast and selective method for monitoring the neurotoxin.

Non-enzymatic methods

Different non-enzymatic methods for the determination of ODAP were reported [18-24]. However, all are found to be nonselective and experimentally inconvenient. The most widely used method for determining the neurotoxin in foods and seed samples, originally described by Rao, utilizes the reaction of o-phthalaldehyde (OPT) with L-α,β-diaminopropionic acid, DAP, formed on hydrolysis of both the α- and the β-isomers of ODAP and measurement of absorbance at 420 nm [18]. This method, however, has got several limitations. It is a batch method which requires an extraction time of 6 hr and a 1-hr sample pretreatment prior to the final determination [18]. An additional disadvantage is that the method is not selective as the non-toxic isomer, α-ODAP, also hydrolysis to the same product. Isomerization of the toxin to the α-form occurs at neutral pH and higher temperatures to a level of about 60% [19, 20]. The need for β-isomer selective method is, therefore, clearly evident.

An attempt to separate α- and β-ODAP with copper chelation has not been very successful since the method does not give sufficiently pure separation of the α-isomer [21]. High performance liquid chromatographic (HPLC) detection methods for ODAP, in which all of them are based on off-line pre-column derivatization, have been reported recently [19, 22-24]. Apart from the experimental inconvenience of separating the reagent solvent after derivatization, the methods are not fast (sample throughput: 8-40 min per sample). Derivatization with dansyl-Cl and 9-fluorenylmethyl chloroformate (FMOC) are suitable for detection of both α- and β-ODAP in the picomolar range, but the methods do not resolve the two components [22, 23].

Enzymatic methods

Enzymes are proven analytical reagents for fast and selective analysis of biological compounds. The enzyme DAP-ammonia lyase (from *Pseudomenad Sp.*) was used for the determination of ODAP after its alkaline hydrolysis to DAP [25]. This assay is evidently unselective as the method of Rao. Very recently glutamate oxidase, GIOD, (from *Streptomyces Sp.*) has been found to catalyze the oxidation of β-ODAP selectively [26] and the oxidation products, hydrogen peroxide and ammonia are detected. To minimize the high cost of analysis, the enzyme was immobilized and based on the immobilized GIOD reactor as a biocatalyst, a relatively very fast flow injection method (FI) (sample throughput: 20 samples per hour) for the toxin in LS has

been developed recently. The FI system involved three other interference-eliminating and indicator enzyme reactors [27]. The new method is evidently an important progress towards ODAP analysis, particularly in monitoring a large number of samples from the field. Unlike liquid chromatographic methods, there is, of course, no separation time needed and the speed of an enzyme-based flow injection system can be designed so that it depends on the enzyme loading in the reactors.

An effective separation of the protein from *lathyrus* extracts has to be developed because this is the major disadvantage behind the newly reported flow injection enzymatic determination of ODAP. In the reported method [27], protein separation from the extract was effected by ultra-filtration method which is not commonly available in ordinary labs of the countries directly affected by lathyrism. Alternative methods such as precipitation and solid phase extraction (SPE) will have to be tested to this effect.

Thus, the objectives of this investigation are:

1. To make kinetic studies of the effects of concentration, temperature and pH on the isomerization reaction of β-ODAP to α- ODAP

2. To optimize methods for separating the protein from lathyrus extracts so that the life time of the reactor will be prolonged

3. To establish the flow injection method for ODAP determination in several sample seeds of *lathyrus sativus* and make comparisons with the colorimetric method developed by Rao.

Chapter 2

REVIEW OF LITERATURE

2.1 ENZYMES

Enzymes are proteins, i.e., they are made up of a complex three dimensional structure of one or several polypeptide chain(s). A large number of enzymes also contain nonpeptide constituents, e.g., a considerable amount of carbohydrate residues. Many enzymes require the presence of a non-peptide compound called cofactor for their catalytic activity. The cofactor can be an organic molecule (coenzyme) or a metal ion. The cofactor can be tightly bound to the enzyme (prosthetic group) or can be added to the system (e.g., nicotinamide adenine dinucleotide, NADH). Enzymes have amino and carboxyl groups, the charges of which vary with the pH. The catalytic ability of the enzymes depends consequently on pH, and presence of ions, since the charge affects the conformation of the enzyme and its electrostatic interaction with substrates.

Like any catalyst, an enzyme accelerates the rate of a chemical reaction by reducing the Gibb's energy of activation, i.e., $\Delta G'^{*}_{E} < \Delta G'^{*}$, where the first term represents Gibb's energy of activation in the presence of an enzyme, and the second without enzyme. Since Gibb's energy has enthalpic ($\Delta H'^{*}$) and entropic ($\Delta S'^{*}$) components ($\Delta G'^{*} = \Delta H'^{*} - T\Delta S'^{*}$), the decrease in the Gibb's energy of activation of catalytic reactions is due to a decrease in enthalpy or an increase in entropy, during the initiation of the reaction [28].

There exist an overwhelmingly large number of methods that utilize enzymes for analytical purposes [29, 30] with clinical or medical significance. The most important reasons for using enzyme mediated reactions in analytical chemistry are the selectivity and the high catalytic rate. The high selectivity is particularly important when complex sample mixtures, e.g. biological samples, are analyzed. This high selectivity of enzymes to a particular substrate(s) can be attributed to a stereochemical complementarity of the active site towards the substrate (lock-and-key hypotheses). This hypothesis explains many features of enzyme specificity but takes no account of the known flexibility of proteins. X-ray diffraction analysis and various spectroscopic data have shown that the free enzyme and the enzyme-substrate complex have

conformational differences. Due to the binding of the substrates, a structural rearrangement of the enzyme may occur as a result of which another part of the enzyme becomes available and can interact with a different part of the substrate (induced-fit hypotheses) [28]. The induced-fit hypothesis essentially requires the active site to be floppy and the substrate to be rigid, allowing the enzyme to wrap itself around the substrate, in this way bringing together the corresponding catalytic site and reacting groups.

The huge number of enzymes has necessitated the introduction of a systematic nomenclature. The systematic names and numbers, which were introduced by the International Commission of Enzymes in 1956 and have been extended by the Enzyme Commission of the International Union of Biochemistry (1961 and 1975), are based on the catalyzed chemical reaction [28]. Six different types of enzyme catalyzed reactions can be distinguished: (1) oxidation reduction; (2) functional group transfer; (3) hydrolysis; (4) lysis; (5) isomerization; (6) ligation. Lysis reactions involve a nonhydrolytic removal of a group resulting in the occurrence of double bonds. Ligation is the combination of two species with concomitant consumption of energy, provided by the breakdown of a pyrophosphate bond in a nucleoside triphosphate. Likewise, enzymes are classified into six main groups: (1) oxidoreductases; (2) transferases; (3) hydrolases; (4) lyases; (5) isomerases; and (6) ligases.

Certain enzymes may have particular group-specificity to a class of compounds with some structural relationship, e.g. common functional group and stereoisomerism [28]. For example , alcohol dehydrogenase catalyze the oxidation of a variety of alcohols; hexokinase assist the transfer of phosphate from ATP to several different hexose sugars; L-amino acid oxidase mediates the oxidation of L-amino acids to oxo acids while D-amino acid oxidases catalyzes the oxidation of D-amino acids.

The enzyme glutamate oxidase, GIOD, identified by Kusakabe and coworkers [31], has been reported to be almost specific to the oxidation of L-glutamate, only with 0.6% relative activity to L-aspartate at pH 7.4 [31]. They reported that none of the other essential amino acids were oxidized by the presence of the enzyme. Recently Moges and coworkers [26] have shown that this enzyme catalyzes the oxidation of the neurotoxin β-ODAP found in LS. The relative activities of this enzyme to glutamate, ODAP and aspartate at pH 7 and room temperature are 100, 0.8 and 0.3% respectively [26]. These two reports [26, 31] strongly indicate that the presence of an

additional (terminal) carboxylic group other than the α- carboxylic group is essential for the activity of the enzyme. The three amino acids have the following structure and the percentage in brackets is relative activity of GIOD with respect to each substrate.

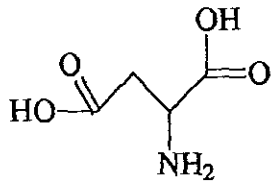

Aspartate (0.3%)

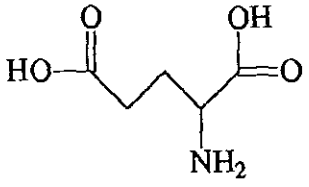

Glutamate (100%)

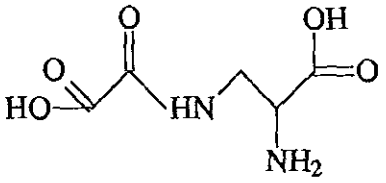

ODAP (0.8%)

2.2 IMMOBILIZED ENZYMES

An immobilized enzyme is one which is attached to a solid support (by covalent binding or physical adsorption), enclosed by an insoluble support (termed a **carrier**), or one where the enzyme molecules have been cross-linked to each other, without significant loss of catalytic activity.

Enzymes are immobilized for a number of reasons. The first and most obvious advantage is that enzymes can be physically separated from reaction mixtures in their immobilized form and consequently be reused. This evidently reduces the cost of enzymatic analysis. As a general rule, immobilization of enzymes is considered to be a successful procedure for increasing their stability, because they resist inactivation under denaturation conditions [32]. Additional advantages obtained by immobilizing enzymes are favourable storage, operational and thermal stability, extended pH range for the performance of the enzyme. Different support materials are available to immobilize an enzyme. The choice of the support material for enzyme immobilization depends on several factors such as the interaction between the carrier and the enzyme, which may have an influence on the stability and kinetics, the capacity of the carrier to bind protein, the surface charge and hydrophilicity, the dimensional and chemical stability, the ease of activation, the interaction of the support with the analyte or sample matrix, and the cost, regenerability and availability. Methods of immobilizing enzymes are: adsorption, ion-exchange, entrapment, cross-linking, microencapsulation and covalent attachment [28-30, 32, 33].

Physical adsorption to an inert support is a very simple experimental procedure for immobilizing enzymes. An enzyme solution is brought in contact with an adsorbent followed by washing the resulting conjugate to remove any non-adsorbed enzyme. The main disadvantage is desorption of the enzyme if the binding between the enzyme and the support is too weak. This results in a loss of catalytic activity and contamination of the product.

Enzymes can also be physically entrapped in the interstitial space of water-insoluble polymers and thus cannot easily permeate out of the gel matrix. Substrate and product can, however, permeate across and within this gel matrix. This method permits the preparation of water-insoluble derivatives of widely different physical forms.

In microencapsulation, the enzyme can be immobilized within microcapsules which have either a permanent or non-permanent semipermeable membrane. This technique allows the immobilization of different enzymes in one step. The main disadvantages are leakage and enzyme deactivation.

Intermolecular crosslinking using multifunctional reagents such as glutaraldehyde is an effective way to immobilize enzymes. The reaction between glutaraldehyde and protein is fast [34] and usually complete within an hour. This technique demands fairly stringent controls, e.g., on pH, concentrations, etc. in order to achieve efficient insolubilization, and requires large amounts of proteins or co-proteins. Crosslinked immobilized enzymes have nevertheless some advantage in that leakage is prevented, and enzyme stability is improved. Disadvantages of this approach are that experimental conditions must first be determined to ensure optimum attachment of the enzyme onto the support. Moreover, the often unavoidable inactivation of the enzyme caused by chemical modifications, and the gelatinous nature of these enzyme derivatives, makes them difficult to use in column operations.

Immobilization of enzymes by means of covalent coupling to a reactive insoluble support, e.g., porous glass, or to an electrode surface is the method of choice if a long operational performance is required. Porous glass is first silylated to alkylamino or arylamino derivatives to which the enzyme can be bound by reaction with e.g. glutaraldehyde, isothiocyanate, carbodiimide, triazine, or azo coupling [30, 35]. Glutaraldehyde was used in this work. Covalent coupling gives rigid structure for the enzyme that may lead to an increased stability preserving the native

conformation of the protein and making unfolding less probable [36, 37].

Analytically, the advantages of enzyme immobilization are overwhelming in that continuous analysis and automation are easier to accomplish and it is less time consuming compared with the conventional enzyme batch method. One disadvantage of immobilizing an enzyme is that the specific activity of the immobilized enzyme is usually lower than that of the corresponding soluble enzyme since some portion of the enzyme molecule that might be necessary for the full activity may be immobilized. Nevertheless, the loss in specific enzyme activity due to immobilization can be counteracted by increasing the immobilized enzyme to substrate ratio, i.e., using large enzyme reactors/small injection volumes.

Analytical applications of immobilized enzymes have followed two main lines [38-42]. The first is the immobilized-enzyme reactor (IMER) in which the effluent of the reactor in flow system is coupled with some kind of detection system such as a spectrophotometer or electrode system. The second is a biosensor in which the enzyme is immobilized in close proximity to a physical transducer (detector) such as an electrode. Comparatively, enzymes immobilized in a reactor seem more stable than when they are immobilized in close proximity to an electrode surface. A strict comparison, in relation to the different environments and the conditions of the enzyme on an electrode and in a reactor, however, cannot be made since reactors usually have high enzyme loading while electrodes offer a limited surface for enzyme immobilization. Some obvious advantages can be obtained by immobilizing enzymes in reactors. The amount of enzyme that can be immobilized and contained in a reactor of moderate size is very large as a result when a solution containing the enzyme substrate passes the reactor, equilibrium of the enzymatic process can be reached. In cases where the equilibrium strongly favours the product side, virtually 100% conversion of the substrate into a detectable product can be achieved. Furthermore, in a reactor with high enzyme loading a slight variation in the flow rate, pH, ionic strength, temperature, and small concentration of inhibitors and activators will not affect the conversion efficiency [41].

2.2.1 IMMOBILIZED ENZYME REACTORS (IMERs)

IMERs have found numerous applications since their introduction by Reisel and Katchalski twenty years ago [43]. They can easily be interphased with almost any

type of detector which can record the concentration of the substrate, a product, a cosubstrate, or a coenzyme. Their utility can be increased by mounting different enzyme reactors in series or by co-immobilization of two or more enzymes. The attainable conversion efficiency which will impose the sensitivity of the analysis may differ widely depending on the reactor configuration used. The most commonly used reactor configurations are: packed-bed reactors, single-bed-stirring reactors (SBSR), and open tubular heterogeneous enzyme reactors. In the latter, the enzyme is bound on the inner wall of the tube [44]. These type of reactors usually have to be very long since the surface area for enzyme immobilization is low to achieve the required surface area. They are not well suited for FI applications because the sensitivities become too low and the dispersion too high with continuous flow due to the large diameters of the tubes. A compromise between packed-bed reactors and open tubular heterogenous reactors in terms of dispersion, conversion efficiency, and back pressure is offered by the SBSR in which a single stirring of glass beads with the immobilized enzyme is packed into a coiled glass or nylon tubing. However, this reactor type also offers a restricted amount of immobilized enzyme per reactor volume. The packed bed reactor is the most frequently used of the three mentioned and is also the type used for GIOD and GIOD-Catalase reactors described in this report. The enzyme support in the packed bead reactor was controlled pore glass (CPG). A high enzyme loading on the support should be achieved to exhibit a high activity of the bound enzyme.

2.2.2 KINETICS OF IMMOBILIZED ENZYME REACTORS

Enzyme kinetics for immobilized enzyme systems, e.g., immobilized reactors, is commonly assumed to be similar to those of soluble enzymes [45]. However, a clear-cut evaluation of the parameters governing the performance of immobilized enzyme systems will require some understanding of the cooperation of kinetics and mass transfer in immobilized enzyme systems.

The simplest enzyme-catalyzed reaction involves a single substrate binding to the enzyme under the formation of an enzyme-substrate complex, which in turn irreversibly decays to the product and free enzyme.

$$E + S \underset{K_{-1}}{\overset{K_1}{\rightleftarrows}} ES \xrightarrow{K_2} E + P \qquad (2.2.1)$$

The Michaelis-Menten kinetic equation for soluble enzymes, which describes this case and derived under the assumption of steady-state conditions, is

$$-d[S]/d[t] = V_{max}[S]/([S] + K_M) \qquad (2.2.2)$$

where V_{max} is the maximum reaction rate at a particular enzyme concentration and K_M is the Michaelis-Menten constant.

In order for Michaelis-Menten kinetics to apply to enzyme reactors with porous matrices, external and internal mass-transfer limitations have to be taken into consideration [46, 47]. The effective substrate concentration in reactors with mass transfer resistance is less at the catalyst site than in the bulk. The reactor kinetics can therefore be represented by a first-order expression even at concentrations well above the K_M of soluble enzyme; hence equation 2.2.2 takes the form

$$-d[S]/d[t] = K_{ps}^{app} [S] \qquad (2.2.3)$$

where K_{ps}^{app} is the pseudo-first order apparent rate constant identical to V_{max}/K_M^{app} which contains the effects of both internal and external mass-transfer limitations. Integration of equation 2.2.3 over time yields

$$-\ln (1-X) = K_{ps}^{app} \tau \qquad (2.2.4)$$

where τ is the mean residence time for a volume element in the reactor and X the fractional conversion; $X = (S_o-S)/S$.

In order to separate the effect of resistance towards external mass transfer, the following equation has been proposed [46]:

$$1/K_{ps}^{app} = d_p^{3/2} B^{-1} F^{-1/2} + 1/K_{ps} \qquad (2.2.5)$$

where F is the linear flow rate, B a collection of constants containing the molecular diffusion coefficient and the kinematic viscosity, d_p the particle size, and K_{ps} is the rate constant in the absence of external mass-transfer limitations. Separation of the limitations arising from internal mass transfer will require the diffusivity in the pores to be taken into consideration. Equation 2.2.5 shows that the apparent rate constant

for a substrate converting reactor increases with the flow rate in a nonlinear fashion and the limitations imposed by the internal mass transfer affect the apparent pseudo-first order rate constant.

2.3 SEPARATION OF PROTEINS

Proteins are macromolecules with molecular weight of at least several thousand daltons. They are found in abundance in living organisms, making up more than half the dry weight of cells. Two distinct types of proteins are known: fibrous and globular proteins. The former are insoluble in water and are tough, which enables them to play a structural role. Examples include α-keratin (a component of hair, nails and feather) and collagen (the main fibrous element of skin, bone and tendon). In contrast, globular proteins are generally soluble in water and may be crystallized from solution. They have a functional role in living organisms . All enzymes are globular proteins.

Normally protein-containing samples cannot be directly injected on to a FI system because the accumulation of proteins on the surface of the reactor deteriorates its performance. Moreover the accuracy, reproducibility, precision and the selectivity of measurement is decreased. Thus, sample clean-up before injection should be executed. For the separation of proteins from sample mixtures a number of procedures are applied [48-50] such as precipitation of the proteins, isolation of the analyte with a (disposable) solid phase cartridge, (ultra)filtration and dialysis techniques.

Precipitation of proteins from biological samples can be performed with a great number of reagents [48, 50], e.g., organic solvents like acetonitrile, acetone, ethanol, methanol; acids like trichloroacetic acid, perchloric acid, tungstic acid, hydrochloric acid; salts such as ammonium sulphate and ammonium chloride. Applying inorganic salts (ammonium sulphate or ammonium chloride), a reversible protein precipitation is achieved, meaning that after dilution of the samples the biological activity of the proteins is still present. However, use of acids or organic solvents for protein precipitation destroys the biological activity of the proteins irreversibly.

The use of solid phase extraction for sample pre-treatment has gained increased popularity during the last decade because it is efficient, fast and easy to automate [51]. The extraction procedures are relatively simple; a disposable manually packed or prefabricated cartridge with a suitable sorbent is solvated (wetted) and conditioned

with appropriate solvent and the sample is applied. The wetting, especially for the chemically bonded hydrophobic columns, is very important because it opens the hydrocarbon chains (solvation) and increases the surface area of the sorbent [51]. Subsequently the column is washed, and the analyte(s) are eluted selectively from the column with less than 1 ml of the isolation solvent. Elution of the analytes can be executed with reduced pressure, syringe, or by centrifugation.

Ultrafiltration is based on the selective retainment of analytes by convective solvent flow through an anisotropic membrane. Compounds with dimensions larger than the specified membrane molecular cut-off are nearly quantitatively retained and compounds with smaller dimensions pass the membrane together with the solvent. Nowadays ultrafiltration membranes are present with cutoff values ranging from a molecular weight of 500 to 300,000. To achieve the desired ultrafiltration, the equipment must be designed to obtain a high transport flow rate over the membrane and to diminish the effect of concentration polarization (increase of macromelecular concentration just above the membrane), which is the major problem in ultrafiltration. This technique was used by Moges and Johansson [27] to separate proteins from LS extracts.

In dialysis the analytes are separated from the sample matrix by diffusion through a semi-permeable membrane. Usually a porous membrane, clamped between two blocks each of which contains a flow channel, is used. As membrane material, polymers such as cellulose or acetylated cellulose are often used. The diffusion across the membrane is a rather slow process, driven by the concentration gradient of the analyte, and accordingly, when the concentration in the acceptor (receiving) solution equals that of the donor (sample), the net flux will be zero. This technique is not very selective, and two analytes can be separated only if their molecular sizes, and thus their fluxes, are substantially different. On the other hand, the isolation from macromolecules is very efficient, and applications are often found in the biomedical field as a clean-up of plasma samples. As dialysis leads to sample dilution, a subsequent concentration step is often needed. This can often be achieved by adding a pre-column prior to the analytical column.

2.4 FLOW INJECTION ANALYSIS (FIA)

FIA constitutes the most advanced form of solution manipulation available to analytical chemists for the mixing and transport to the measurement point of sample reagents and products of one or more chemical reactions. FIA has created a revolution in analytical methodology, assisted by the availability of instrumentation directed at mechanization and automation of routine operations which were undertaken manually.

The concept of FIA received earliest attention from the electrochemist. Nagy, Feher, and Pungor published a paper in 1970 describing injection of a sample into a flowing stream of electrolyte [52]. Their system involved passage of the sample carrier stream through a magnetically stirred mixing chamber followed by flow past a silicone-rubber-based graphite electrode. The resulting analytical readout was in the form of transient peaks.

Subsequently, Ruzicka and Hansen in Denmark [53] and Stewart and co-workers in the United States [54] simultaneously modified the technique in the mid-1970's. Their primary innovation was in the use of flow-induced sample dispersion as the sample carrier stream was pumped through narrow bore tubing. This mechanism was used to effect controlled mixing of the sample with the reagent stream as opposed to the gross mixing generated in the mechanically stirred chamber, thereby avoiding excessive sample dilution.

FI methods are an out growth of air segmented-flow analysis (SFA), which were widely used in clinical laboratories in the 1960's and 1970's for automatic routine determination of a variety of species in blood and urine samples. In SFA, samples were carried through the system to a detector by a flowing aqueous solution that contained closely spaced air bubbles. The purpose of the air bubbles was to prevent excess sample dispersion, to promote turbulent mixing of samples and reagents, and to scrub the walls of the conduit, thus preventing cross-contamination between successive samples. However, the presence of the air bubbles in SFA poses several problems. The inherent compressibility of the air bubbles causes the system to pulsate and give rise to a lag in recording the signal. The system requires the use of certain mechanisms for the reproducible introduction (aspiration) and removal (deaeration) of the bubbles. Moreover, the flow rate is more difficult to control in the presence of air bubbles, partly because of the various types of interaction possible between air and the materials encountered in an SFA assembly.

The discoverers of FIA found, however, that excessive dispersion and cross-contamination are nearly completely avoided in a properly designed system without air bubbles and that reproducible mixing of samples and reagent could be easily realized [55].

2.4.1 PRINCIPLES

FIA is based on the introduction of a liquid sample into a moving, nonsegmented continuous carrier stream of a suitable liquid. The injected sample forms a zone, which is then transported towards a detector that continuously records the absorbance, electrode potential, or other physical parameter as it continuously changes due to the passage of the sample material through the flow cell.

The simplest flow injection analyzer (Fig.1) consists of a pump, which is used to propel the carrier stream through a narrow tube; an injection port by means of which a well-defined volume of a sample solution is injected into the carrier stream in a reproducible manner; and a microreactor in which the sample zone disperses and reacts with the components of the carrier stream, forming a species that is sensed by a flow-through detector and recorded. A typical recorder output has the form of a peak (Fig.2) the height H, width W, or area A of which is related to the concentration of the analyte. The time span between the sample injection S and the peak maximum, which yields the analytical readout as peak height H, is the residence time T during which the chemical reaction occur.

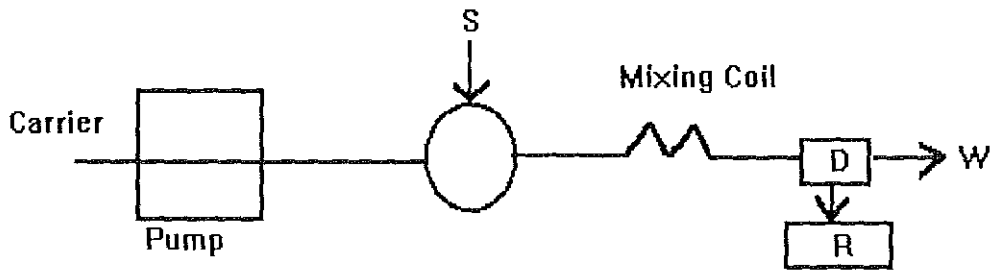

Fig.1 The simplest single-line FIA manifold utilizing a carrier stream of reagent; S is the injection port, D is the flow cell, R is the recorder and W is the waste.

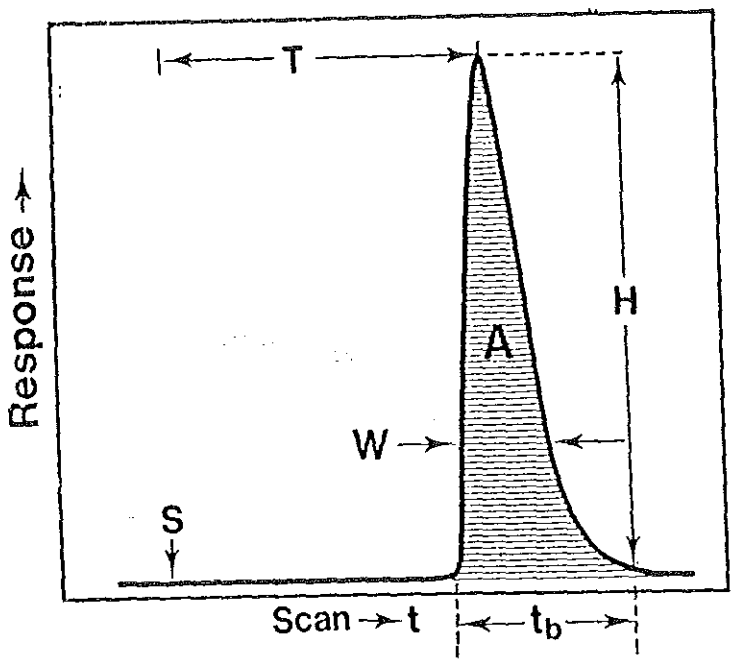

Fig.2 Typical detector out put of an FIA system, the recording starting at S (time of injection t_o). H is the peak height, W is the peak width at a selected level, and A is the peak area, T is the residence time corresponding to the peak height measurement, and t_b is the peak width at the baseline.

FIA is based on a combination of three principles: *sample injection, controlled dispersion of the injected sample zone,* and *reproducible timing* of its movement from the injection port toward and into the detector. Thus, in contrast to all other methods of instrumental analysis, the chemical reactions are taking place while the sample material is dispersing within the reagent, that is, while the concentration gradient of the sample zone is being formed by the dispersion process. The concept of dispersion, therefore, controlled within time and space, is the central issue of FIA.

2.4.2 DISPERSION

During its transport towards the detector, the sample forms a zone which disperses in a very reproducible way, and makes the analytes react with the reagents in the carrier (or with a reagent-surface). Due to the dispersive forces imposed by the flow, the sample zone becomes broadened and diluted during its passage from the injector to the detector.

In order to design an FIA system rationally, it is important to know (a) how

much the original sample solution is diluted on its way toward the detector and (b) how much time has elapsed between the sample injection and readout. For this purpose, Ruzicka and Hansen [55] defined the dispersion (D) as the concentration of the sample zone at the time of injection (C^o) divided by the concentration of the dispersed sample zone entering through the detector (C^{max}). The peak height (h) is proportional to the sample concentration and can be used to evaluate the dispersion in the FI system provided a linear response curve is at hand. The integrated peak area is proportional to the amount of injected sample and should evidently be constant at all times.

$$D = C^o/C^{max} \propto h^o/h^{max} \qquad (2.4.1)$$

A major aim in FIA is to combine a high sensitivity and a high sample frequency with as low as possible reagent and sample consumption. Consequently, peak broadening and hence dispersion should be minimized.

The sample solution, when D = 2, for example, has been diluted 1:1 with the carrier stream. For convenience, sample dispersion has been defined as limited (D = 1-3), medium (D = 3-10), and large (D > 10), and the FIA systems designed accordingly have been used for a variety of analytical tasks.

Limited dispersion is preferred when measuring the property of the analyte directly in the absence of process other than transport. Since the residence time is rather short, convection will prevail over radial diffusion. Therefore, to minimize dispersion these systems must adopt (a) a high flow rate (> 2 ml/min), (b) a large sample volume, and (c) a small reactor volume. Application of these conditions affords high sampling rates and better analytical sensitivity than attained in ordinary FIA systems. Typically, atomic-absorption spectrophotometer or a flow-cell with electrode (pH, ISE) for direct potentiometric sensing are used as detectors in such systems.

Medium dispersion is employed when the analyte must mix and react with the carrier reagent to form a product to be detected. It is therefore necessary to effect partial mixing between the injected sample zone and the stream containing the reagent. This can be accomplished by using long tubes, low flow-rates, several channels with various mixing points, etc.. Detection is usually by photometric or

fluorometric means. Sample throughput and sensitivity are generally lower than the previous class of systems.

Large dispersion is used only when the sample must be diluted to bring it into measurement range. In such cases the residence time is rather long, so in some cases chemical equilibrium is attained. These systems incorporate either a mixing minichamber with a stirrer or a very long reactor tube. These are not the common conditions in FIA. Their application is restricted to FIA titration and some other gradient modes of operations [55]

The simplest way of measuring the dispersion coefficient is to inject a well-defined volume of a dye solution into a colourless carrier stream and to monitor the absorbance of the dispersed dye zone continuously by a colorimeter. To obtain the D^{max} value, the height (i.e., absorbance) of the recorded peak is measured and then compared with the distance between the baseline and the original signal obtained when the cell has been filled with the undiluted dye. Provided that the Beer-Lambert's law is obeyed, the ratio of respective absorbances yields a D^{max} value that describes the FIA manifold, detector, and method of detection.

The FIA peak is a result of two kinetic processes, which occur simultaneously; the *physical* process of zone dispersion and the *chemical* process resulting from reactions between sample and reagent species. The underling physical process is well reproduced for each individual cycle; yet it is not a homogeneous mixing, but a dispersion, the result of which is a concentration gradient of a sample within the carrier stream.

2.4.3 FACTORS AFFECTING PEAK HEIGHT

The degree of dispersion, and therefore the recorded peak height, is determined by a number of factors, including injected sample volume, channel geometry and length, and flow rate.

1. ***SAMPLE VOLUME.*** Consider a one-line FIA system in which the pumping rate Q is 1.5 ml/min, the tube length L is 20 cm, and the inner diameter of the tube is 0.5 mm. When increasing volumes of a dye solution are injected, a series of curves, all starting from the same point are recorded. The height of the individual peaks will increase until an upper limit "steady state" has been reached. At this final level the

recorded absorbance will correspond to the concentration of undiluted dye C^o, and D = 1. The rising edges of all curves coincide and have the same shape regardless of the injected volumes, and thus:

$$C^{max}/C^o = 1 - \exp^{(-kSv)} = 1 - \exp^{(-0.693n)} = 1 - 2n = 1/D^{max} \qquad (2.4.2)$$

where $n = S_v/S_{1/2}$ and $S_{1/2}$ is the volume of sample solution necessary to reach 50% of the steady-state value, corresponding to D = 2. 75% of C^o is reached when two $S_{1/2}$ volumes are injected which correspond to D = 1.33. Therefore, D = 1 can never truly be achieved; yet, injection of five $S_{1/2}$ volumes results in D = 1.03, and injection of seven $S_{1/2}$ volumes result in D = 1.008, corresponding to 99.2% of C^o. As the concept of steady-state is not used in FIA, the maximum sample requirement will not exceed two $S_{1/2}$ for limited dispersion, and less than one $S_{1/2}$ in all other applications. Since the first portion of the rising curve might be considered nearly linear up to approximately 50% C^o (i.e., D = 2), it follows that for FIA readouts with medium and large dispersion coefficients, the peak height is directly proportional to the injected volume. Therefore, changing the injected sample volume is a powerful way to change dispersion. An increase in peak height-and in sensitivity of measurement-is achieved by increasing the volume of the injected sample solution. Conversely, dilution of overall concentrated sample material is best achieved by reducing the injected volumes [55].

It has been shown that $S_{1/2}$ does not depend on the method of injection (valve injection or impulse injection), but is a function of the geometry and of the volume of the flow channel [56].

2. ***CHANNEL LENGTH AND FLOW RATE.*** The microreactor between the injection port and the detector may have different lengths, diameters, and geometries. The effect of coil length L and inner diameter of the tubing d on the dispersion has been studied in detail [55]. The use of tubing of a small diameter will result in lower $S_{1/2}$ values, because the sample will occupy a longer length of tube (θ), i.e., the sample will be less easily mixed and dispersed. The sample volume S_v injected is equal to $\prod R^2\theta$. If the tube diameter d is halved, the sample will occupy a forth fold-longer portion of the tube (θ), and, hence, the $S_{1/2}$ value will be four times smaller.

Therefore, if a limited dispersion is desired, a sample volume of a minimum of 1 x $S_{1/2}$ should be injected into a manifold consisting of the shortest possible piece of a narrow tube connecting the injection port and the detector.

Even if a medium dispersion FIA system is required, it is economical to use narrow channels. The sample and reagent economy is improved when narrow channels are used, because for the same linear flow rate, the pumping rate Q in a tube of diameter d is only one-forth of that required for a tube of diameter 2d. On the other hand, practical considerations prevent the use of channels with too narrow a bore or too tightly packed reactors because:

1. The flow resistance will increase, thus preventing the use of a low-pressure drive
2. The system might easily become blocked by solid particles, which will make its use impractical for assay of clinical, agricultural, and similar sample materials unless the samples are meticulously filtered in a preliminary step.
3. The use of manifold tubing narrower than flow cell diameters will cause an undesired non uniformity in the flow pattern in the detection area.

Generally, the optimum internal diameter of tubes connecting the injection port and the detector is 0.5 mm, although 0.75 mm inside diameter is useful for the construction of systems with large dispersion.

The mean residence time, T_{mean}, will depend, for a reaction system made of tubing of uniform internal diameter, on the tube length L, the tube diameter d and the pumping rate Q:

$$T_{mean} = \prod R^2 L/Q = L/F = V_r/Q \qquad (2.4.3)$$

where F is the linear flow rate and V_r is the reactor volume. Thus, when designing systems with medium dispersion where the sample has to be mixed and made to react with the components of the carrier stream [56], one would tend to increase the tube length L in order to increase T_{mean} and thus T. However, increasing of the tube length increases the distance travelled by the sample zone. As a result the dispersion of the sample zone increases and this band broadening will eventually result in loss of sensitivity and lower sample throughput. It has been shown [55-58] that dispersion in a FIA system caused by the flow in the open narrow tube increases with the square root of the mean residence time T_{mean} (or the distance travelled, L) and that for constant flow velocity the residence time is proportional to the dispersion to the second power:

$$D_{max} = 2\pi^{3/2}R^2D_f^{1/2}T_{mean}^{1/2}/S_v \qquad (2.4.4)$$

where D_f denote al dispersion coefficient and R is the tube radius.

Thus, ev h the sample broadening becomes progressively smaller relative to the ravelled, the increase in T obtained through an increase of length L (for i dispersion) is not worthwhile above a certain limit. It is desirable to ke t for narrow peaks and for rapid throughput. Because of the physical distar veen the individual components of the FIA system (injection port, reaction w through cell), a compromise must be made, and therefore, in practice, th length of a well-designed FIA manifold is between 10 and 100 cm of 0.5 m . Residence times up to 20 sec can readily be obtained by selection of t ate, and longer residence times may be obtained by means of intermittent

3. ***CHANNE IETRY***. Straight tube, coiled tube, mixing chamber, single-bead reactor, 3-D tted" reactor and imprinted meander or combinations of these geometries used for the FIA microreactor [55]. These reactors are used to increase th ty of radial mixing, by which the parabolic velocity profile in the axial dire ned when the sample zone is injected into a laminar flow of carrier stream, . As a result, the reagent becomes more readily mixed with the sample ial dispersion of the sample zone is reduced.

A coiled tube is the most frequently used reactor geometry since it can conveniently accommodate any length of tubing in an experimental set up and also because secondary flow within the coiled tubing promotes mixing in the radial direction. The result is a more symmetrical, higher, and narrower peak than if an identical tube length had been used. The tighter the coiling of the tube is, the more pronounced this effect will be [59]. The longer the tube is, the larger the number of mixing stages can be accommodated and the more symmetric the peak obtained will be.

2.4.4 ANALYTICAL APPLICATIONS OF IMERS IN FIA

One of the great advantages of the FIA technology is the ease with which additional components can be added to the system to achieve a particular analytical

objective. On-line components in FIA may perform, for example, pre-concentration, separation, extraction, reagent generation, reactions for the determination of analytes, and interference elimination [55]. Where appropriate the latter two can be rendered using enzyme reactors.

Single analyte determination. The most common and the simplest application of an enzyme reactor is its use in single analyte determinations [30, 41, 55] provided the analyte reacts with the enzyme to produce detectable species. Two or more enzymes may be used in one reactor (co-immobilized enzymes) or, alternatively, another reactor may be inserted between the analytical reactor and the detector to indicate the reaction.

The use of enzyme recycling reactions has led to the development of highly sensitive measuring systems with low detection limits. Signal amplification is observed in cases when, for two coupled enzymes, the product of one enzymatic reaction can be cycled back by another enzyme to the original substrate. The substrate can thus be recycled many times in the reactor. The sensitivities attained with recycling reactions can therefore become very high. The amplification depends on the rate and the period of the reaction, i.e., enzyme loading and residence time of reactants for an enzyme reactor in a flow system. Appropriate selection of the enzymes that play this role can be made based on existing kinetics data. A recent example describing such a case is an FI system for a substrate recycling of NAD^+/NADH with an enzyme reactor containing co-immobilized glycerol dehydrogenase and diaphorase [60]. In this system, glycerol is oxidized by NAD^+ and the NADH formed is re-oxidized back to NAD^+ by diaphorase in presence of hexacyanoferrate(III). The reaction was monitored by amperometric detection of the product, hexacyanoferrate(II), at a glassy carbon electrode held at 350 mV vs SCE. At a flow rate of 0.5 ml/min, an amplification factor of 175 was obtained. With a stopped flow of four min, the signal increased another 88 times, resulting in a signal amplification of 15,400 times.

Multi-analyte determination. Two or more analytes in the same sample can be determined, either simultaneously or sequentially, in FIA using different combinations of reactors. In simultaneous determination of analytes, the sample carrier stream is divided into as many lines (equal to the number of analytes) before reaching the first

analytical reactor and merge again at a confluence point for reaction in the indicator reactor. Delay coils are inserted in the divided lines so that the reacted sample components reach the detector at different time intervals resulting in different signals. Massom and Townshed [61] determined glucose and fructose simultaneously using invertase-mutarotase (Inv-Mut) and glucose oxidase (GOD) reactors. The signal of the sample portion which will pass through both the Inv-Mut GOD reactors will represent the total response to both analytes, while the detector signal for the sample passing through the delay coil (to the GOD reactor) will be to glucose only. The concentration of sucrose is then determined by subtracting the concentration of glucose from the total. A number of such techniques for the determination of many analytes present in the same sample are reported [62-63].

N number of analytes in a sample can sequentially be determined from N injections of the same sample. In this method, one or several injected samples are subjected to one or several detection points at different times. When one detector is used for sequential determination of analytes, the injected sample is made to split into a number of subplugs, each routed through individual reactors of different lengths, the streams subsequently being combined *via* a confluence point so that the sample subplugs reach the detector sequentially. Moges and Johansson [64] demonstrated sequential determination of creatine and creatinine using packed bed enzyme reactors under equilibrium conditions in FIA. Several detection points can also be used to obtain sequential analytical signals; the detectors-either of the same or different kind-can be located in parallel or in series.

Interferant-eliminating reactors. One very useful application of enzyme reactors in flow systems is in the efficient destruction of interfering species in a sample. A compound that may contribute to the detection signal with or without participation in the analytical or indicator reaction can be catalytically destroyed, with an appropriate pre-reactor, to give non-detectable species. Review of the usual types of interferences and the pre-reactors used in eliminating such compounds is given in [65].

If the reagent stream contains a substrate which is identical to the analyte, a reactor may be inserted along the reagent channel to destroy this undesired component. In this connection an on-line removal of dissolved oxygen in a reagent carrier was made by Yang [66] in FI system for the determination of oxygen using a

Mut-GOD-based amperometric biosensor. A sample is injected after a carrier (glucose in phosphate buffer) passes through a Mut-GOD-Cat reactor to catalytically destroy dissolved oxygen.

An enzyme which has two or more substrates may also be used to determine one of the substrates in a sample if an on-line elimination method can be designed for undesired substrate(s). An example is hexokinase which catalyzes the transfer of phosphate to both fructose and glucose from ATP. Selective determination of fructose in a mixture containing fructose and glucose with hexokinase and glucose isomerase-G6PDH reactors, after an on-line destruction of glucose using a pre-reactor consisting of Mut, GIOD and Cat was reported [67].

If the difference between the reaction rates of two substrates, catalyzed by the same enzyme, is sufficiently wide, interference of the substrate to which the enzyme is more reactive can be eliminated using a small reactor. The catalytic activity of GIOD to ODAP is much lower than to the main substrate, glutamate [27]. Thus interference from glutamate in the FI assay of the toxin, β-ODAP, can be removed using a small GIOD pre-reactor (followed by the destruction of the hydrogen peroxide produced in a Cat reactor), while most of the ODAP in the sample is unaffected and is available for the subsequent detection reactions [27]. In this work too, β-ODAP from LS seed extracts was determined in a FI system following the same combination of reactors as in [27] but here equal amounts, each 25 μl, of immobilized Cat and GIOD were mixed and added to the same 50 μl reactor.

2.5 DETERMINATION OF HYDROGEN PEROXIDE

The use of enzymes makes it possible to develop very selective and sensitive analytical methods for compounds which otherwise are not readily detected with common methods. A subclass of enzymes trivially known as oxidases, catalyze reactions of substrate molecules, S, by aerobic oxidation with concomitant production of hydrogen peroxide or water depending on the enzyme's ability to donate two or four electrons to molecular oxygen.

$$S + O_2 \xrightarrow{OD} \text{product} + H_2O_2 \qquad (2.5.1)$$

At least forty oxidases that produce hydrogen peroxide are known [68, 69] and several of these have been used for analytical applications. Oxidase catalyzed

reactions are usually monitored by detecting the consumption of oxygen or the production of hydrogen peroxide.

Horseradish peroxidase (HRP) reactors have been used in conjunction with Trinder reagent (based on 2,4-dichlorophenol-6-sulphonate, DCPS and 4-aminophenazone, 4-AP) for flow injection (FI) determinations of hydrogen peroxide and other substrates after reactions in oxidase reactors [26, 27, 70, 71].

HRP, like most peroxidases, is a glucoprotein containing ferriprotoporphyrin IX as the prosthetic group in which the bound metal ion, Fe(III), plays a vital role in the electron-transfer reaction [72]. The enzyme HRP which has been extensively studied as a biological catalyst in analytical systems and the one used in this work will be used to describe the reaction steps when hydrogen peroxide is reduced by substrates.

Generally, HRP reacts according to the following peroxidatic cycle. In a first reaction the cofactor in the enzyme donates a charge equivalent to two electrons to H_2O_2, whereby compound I and H_2O are formed:

$$HRP + H_2O_2 \rightarrow \text{Compound I} + 2H_2O \qquad (2.5.2)$$

This reaction is highly selective in that only a restricted number of peroxide substrates may oxidize the enzyme [72]. The regeneration of the enzyme then occurs in two steps where almost any reducing agent, AH, may donate one electron to compound I, forming Compound II and A:

$$\text{Compound I} + AH \rightarrow \text{Compound II} + A \qquad (2.5.3)$$

A second electron is donated to compound II by AH or a similar compound, recreating the peroxide-active form of the enzyme:

$$\text{Compound II} + AH \rightarrow HRP + A \qquad (2.5.4)$$

As the regeneration of the oxidized cofactor is very unselective, there is a long list of substances (denoted AH) that have been used. Examples are hexacyanoferrate(II), hydroquinone, o-phenylenediamine and ferrocene, all used for electrochemical detection by re-reducing compounds I and II in the regeneration of HRP (reactions

2.5.3 and 2.5.4). Very sensitive chemiluminescent methods with luminol, which require a peroxidase (or other oxidant or catalyst) are also available for many bioanalytical methods [73].

Chromogenic substances whose oxidative products strongly absorb in the visible region of the spectrum are commonly employed in spectrophotometric detections of hydrogen peroxide with HRP as a catalyst. The choice of a suitable chromogen should be based on the requirements for each special case. The selectivity of the method is dependent on factors such as the wavelength maximum and the molar absorptivity of the coloured product as well as resistance towards chemical interferences from other compounds present in the sample matrix.

Many of the classical inorganic chromogens such as titanium(IV)sulphate, iodide, hexacyanoferrate(II) [74], etc. suffer from poor sensitivity or inconveniently low λ_{max} of the coloured product and are thus less suitable for biological samples. These compounds have been replaced by other chromogens of which aromatic amines or aromatic phenols are the most frequently used. The oxidation products are highly coloured and they absorb in the visible region, at wavelengths less susceptible to spectral interferences. These chromogens can be divided into two main groups representing two different reaction types. The first group includes certain types of redox reagents, such as o-dianisidin and 2,2'-azinobis(3-ethylbenzthiazoline-6-sulphonic acid) (ABTS) which upon oxidation give a coloured dimer or a stable radical, respectively. The second group is characterized by oxidative coupling of an aromatic amino compound with another aryl compound. The latter group includes the oxidative coupling of 4-AP or 3-methyl-2-benzothiazolinone hydrazone (MBTH) with either an aromatic phenol or an aromatic amine. One of the reagents first described by Trinder [75] involves phenol and 4-Ap. Phenol was later replaced by DCPS for the determination of glucose using glucose oxidase in which sensitivity improved 4-fold (molar absorptivity = 22,000 m^2 mol^{-1}) at 512 - 514 nm [70]. The quinone imine dye forming reaction is illustrated below.

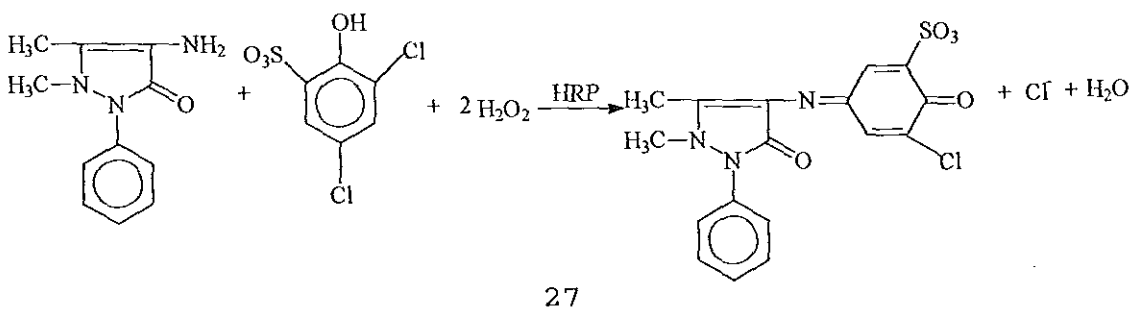

Glutamate oxidase was recently identified as a biocatalyst for the neurotoxic compound, β-ODAP. Its reaction was monitored via Trinder's reaction [26]. The reagent was also used for a FI assay of the toxin in grass pea extracts after its oxidation in a GIOD reactor [27]. The same reagent was used for the kinetic study of the isomerization process of the toxin to the non-toxic and for the determination of β-ODAP in this work.

2.6 KINETICS OF ISOMERIZATION REACTIONS

The direct result of a kinetic study can at best be a rate law, that is an equation showing how the rate of a reaction at a given temperature and in a given medium, varies as a function of the concentration of the reactants. The rate of reaction is expressed as the rate of formation of any product or the rate of disappearance of any reactant. For example, for the hypothetical reaction

$$aA + bB \rightarrow cC + dD \qquad (2.6.1)$$

the rate is expressed as

$$\text{Rate} = -1/a\ d[A]/dt = -1/b\ d[B]/dt = 1/c\ d[c]/dt = 1/d\ d[D]/dt \qquad (2.6..2)$$

The ultimate purpose of a rate study is usually to interpret rate law correctly so as to determine the actual mechanism of the reaction. Mechanism is a specification of what species actually combine to produce the activated complex, and what steps are involved before and after the formation of the activated complex.

The order of a chemical reaction, which is the sum of the powers of reactants in the rate law, can be determined from experimental data using different techniques. Some of the approaches are; the method of integration, the isolation method, the differential method.

Reversible reactions. The simplest case of reversible reactions is that of unimolecular reactions of the type

$$A \underset{k_{-1}}{\overset{k_1}{\rightleftarrows}} B \qquad (2.6.3)$$

If initially, at time t = 0, only A is present then after time, t,

$$[A]_0 - [A] = [B] = X \qquad (2.6.4)$$

The rate law describing this case is

$$dX/dt = k_1[A] - k_{-1}[B] \qquad (2.6.5)$$

which together with equation (2.6.4) becomes

$$dX/dt = k_1[A]_0 - (k_1 + k_{-1})X \qquad (2.6.6)$$

Rearrangement and integration gives

$$\ln\frac{k_1[A]_o - (k_1+k_{-1})X}{k_1[A]_o} = -(k_1+k_{-1})t \qquad (2.6.7)$$

At equilibrium the net rate of the reaction is zero and

$$k_1[A]_e = k_{-1}[B]_e = k_{-1}[X]_e \qquad (2.6.8)$$

where $[A]_e$ and $[B]_e$ are the equilibrium concentrations of A and B respectively and X_e is the value of the conversion variable at equilibrium. Therefore,

$$K = k_1/k_{-1} = [B]_e/[A]_e = X_e/([A]_0 - X_e) \qquad (2.6.9)$$

Substitution of equation (2.6.9) into (2.6.5) gives

$$\ln\frac{(X_e - X_e)}{X_e} \qquad (2.6.10)$$

It follows from equation (2.6.10) that for reversible unimolecular reactions the conversion variable approaches its equilibrium value with a first-order rate constant equal to the sum of the opposing unimolecular rate constants. Knowing the value of the equilibrium rate constant, K, the separate values of k_1 and k_{-1} can be evaluated.

The result is an interesting one. The apparent rate constant is $k_1 + k_{-1}$, which is larger than the forward rate constant. On the other hand, inclusion of the reverse reaction leads to a net reaction rate which is smaller than the forward rate alone, since the net rate consists of a difference of two terms as shown in equation (2.6.5).

The plot of ln $(X_e - X)/X$ against time will be linear and will have an apparent rate constant of $k_1 + k_{-1}$ irrespective of whether the reaction began with pure A or pure B or a mixture of A and B or whether concentrations were such that the particular run proceeded in one direction or the other. An example describing such a case is the cis-trans isomerization of 1,2-dimethylcyclopropane at 453°C [76].

Zero order reactions, though not common, may occur in two situations: when the rate is intrinsically independent of concentration and when the species is in such abundant supply that its concentration is nearly constant during reaction. In the latter case the dependency of the rate on concentration cannot be detected, and apparent zero order prevails.

For a zero order reversible reaction of A to B,

$$A \underset{k_{-o}}{\overset{k_o}{\rightleftarrows}} B \qquad (2.6.11)$$

the differential form of the rate law is

$$-d[A]/dt = k_{app} \qquad (2.6.12)$$

where k_{app} is($k_o - k_{-o}$).
Integration of the above equation with time gives

$$[A] - [A]_o = -K_{app}t \qquad (2.6.13)$$

The distinguishing feature of a zero-order reaction is that the concentration of reactant decreases linearly with time. Examples of homogeneous and heterogenous zero order reactions can be cited from the literature e.g. the decomposition of ammonia on platinum and tungsten surfaces [77], the reaction of acetone with iodine [78] and the decomposition of dinitrogen pentoxide in the presence of nitric oxide [78]. In this work the isomerization of β-ODAP to α-ODAP was found to follow zero order kinetics.

Chapter 3

EXPERIMENTAL

3.1 CHEMICALS AND PREPARATION OF REAGENTS

L-Glutamic acid, L-Aspartic acid, β-ODAP monohydrate (from Sigma) and 4-AP, (BDH) were used as received. Synthesized ODAP.HCl was also used. DCPS was synthesized from 2,4-dichlorophenol (DCP, Merck 3774) and concentrated sulphuric acid according to the method of Barham and Trinder [70] and it was stored at pH 7 in a refrigerator at 4°C. The formation of DCPS was tested spectrophotometrically according to Barham and Trinder [70]. Hydrogen peroxide was standardized by permanganate titration.

The reagent for the FI system was prepared daily in 0.1 M phosphate buffer (pH 7) and consisted of 2.5 mM DCPS, 0.5 mM 4-AP, and 0.5 mM EDTA with 0.25 mM DCP as recommended by Olsson [71] in the presence of 0.02 mg/ml horseradish peroxidase (HRP, E.C. 1.11.1.7, 268 purpurogallin units/mg of solid, Sigma P-8375). The carrier in the flow system was the phosphate buffer.

3.2 IMMOBILIZATION OF ENZYMES

200 mg of controlled pore glass (CPG-10 with 0.12 - 0.20 mm particle size and 51 mm pore size, Serva) was treated with concentrated nitric acid for 2 hr after which it was thoroughly washed with doubly distilled water and dried at 190°C in an oven for an over night. The glass was then silanized by refluxing in boiling water bath with 10% 3-aminopropyltriethoxysilane in dry toluene for 40 min after which it was thoroughly washed with toluene and acetone over a G3 filter and then dried in an oven at 115°C over night. Test on the silanization of the CPG was made by adding 3 - 4 drops of 1.5% 2,4,6-trinitrobenzenesulphonate solution in ethanol into a test tube containing small amount of the derivatized CPG mixed with saturated sodium borate solution. Positive test for the product would give a bright orange coloured surface within about 5 min [79]. The silanized support was activated at reduced pressure and 4°C with 2.5% glutaraldehyde in 0.1 M phosphate buffer at pH 7 for 30 min. The activated support was thoroughly washed with doubly distilled water over a G3 filter. Prior to activation, the stock 25% glutaraldehyde solution (Sigma, G-6257) was mixed

with activated charcoal and centrifuged to remove any possible polymeric product.

400 μl of glutamate oxidase, (GIOD, E.C. 1.4.3.11, 200 units/ml), from Yamasa Corp., Japan, was mixed with 3.5 ml of 0.1 M phosphate buffer at pH 7. The enzyme solution was added to 200 mg of aminopropyl silanized and glutaraldehyde activated controlled pore glass according to a previously described procedure [38]. Based on the absorbance of the enzyme solution before and after immobilization, the coupling yield was 73%. The immobilized enzyme-support was packed in a 250-μl plexiglass tube (i.d. 2.0 mm) and stored at 4°C in 0.1 M phosphate buffer at pH 7 when not in use.

Catalase (Cat, E.C. 1.11.1.6, 19,900 units/mg solid, Sigma C-40) was immobilized on CPG (3 mg/100 mg of glass) using the same method as for GIOD. A mixture of 25 μl each of the immobilized GIOD and Cat was packed in a 50 μl reactor (i.d. 2.0 mm).

3.3 FLOW INJECTION SET UP

Fig.3 shows the assembly of the complete FI system which is a slight modification of the FI system reported recently [27]. It consisted of a two channel peristaltic pump (Gilson Model M 321) which propel the carrier buffer and reagents. Samples were injected from a 20-μl loop with a Rheodyne 7125 injection valve (S). The sample stream (0.3 ml/min), passing through the GIOD/Cat and GIOD reactors, merged with the reagent stream (0.12 ml/min) at a mixing tee (M). The combined reagent and sample streams passed through a coiled tubing (C) to provide effective mixing. The red quinone imine dye formed was then detected at 512 nm in a flow-through cell with an LKB 2151 UV-Vis spectrophotometer (D). The resulting absorption FI peaks were then recorded at a recorder (R). During optimization and in studies of β-α isomerization of the neurotoxin, the 50 μl GIOD/Cat reactor was removed from the system.

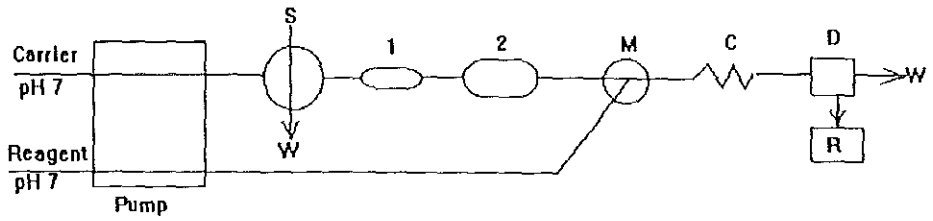

Fig.3 Schematic diagram of the complete FIA manifold for the determination of β-ODAP; reactor 1 (50-μl GlOD-Cat mixture); reactor 2 (250-μl GlOD); the flow rates are 0.3 (carrier) and 0.12 ml/min (reagent).

3.4 ISOMERIZATION STUDIES

A fixed volume of 0.1 M phosphate buffer (pH 7) was introduced into a screw-capped test-tube and heated in a water bath thermostated at 80°C. 10 mM β-ODAP, in the same buffer (also at pH 2), was added to the pre-heated buffer so that the concentration of the compound would be 500 - 2000 μM. Heating continued after inverting the mixture twice (ca. 4 sec). 100 μL sample was withdrawn after one min and added to the same buffer cooled over ice to stop any further isomerization. More samplings were made every five or ten min. Dilutions to the cooled buffer were made to give 200 μM total ODAP. The remaining β-ODAP was determined by injection of the sample at room temperature into the flow system. At least two determinations were made for each sample. Similar experiments were also performed at 60, 70 and 90°C for 1 mM standards (pH 7).

3.5 EXTRACTIONS OF ODAP FROM *LATHYRUS SATIVUS*

β-ODAP, for FI determination, was extracted from 100 mg of grass pea powder in 10 ml of 0.1 M phosphate buffer (pH 7). The extraction was effected over ice bath by agitation with a magnetic stirrer for 2 hr [27]. Particulate matters were separated by centrifugation and filtration through a 0.45-μm membrane filter.

For the colorimetric determination of the toxin using the modified form of the OPT method [80], ODAP was extracted from 80 mg of LS seed powder in 8 ml of distilled water by agitation with a sonicator for an hour. The extraction was made over a water bath thermostated at 50 °C.

Chapter 4

RESULTS AND DISCUSSION

4.1 OPTIMIZATION OF THE FIA SYSTEM

The optimum pH and reagent concentrations for the determination of β-ODAP using a GIOD reactor alone in the flow system were found to be essentially the same as the reported values [27].

The flow rate effect on the carrier and reagent lines was investigated. Since flow rate is inversely proportional to the residence time of the substrates and products within the enzyme reactor [47], decreasing the flow rate will increase the conversion efficiency of the reactor. Hence, there is an optimum flow rate required for equilibrium to set-in, depending on the activity of the enzyme in a reactor. The effect of flow rate in this system was studied by injecting 300 μM β-ODAP into a 20-μl sample loop in the presence of 250-μl GIOD reactor. Data on flow rate studies were obtained with a reagent solution described in the experimental. Fig.4 shows the plot of flow rate against the maximum absorbance. Maximum peak height was obtained for a total flow rate of 0.315 ml/min, but the sample throughput was rather low (about 13 samples per hour). Studies on other variables and calibrations of the system were therefore made at a total flow rate of 0.42 ml/min. The optimum flow rates, 0.3 ml/min for carrier and 0.12 ml/min for reagent, were obtained by using pump tubes of 0.80 and 0.32 cm^2/m for the carrier and reagent streams respectively.

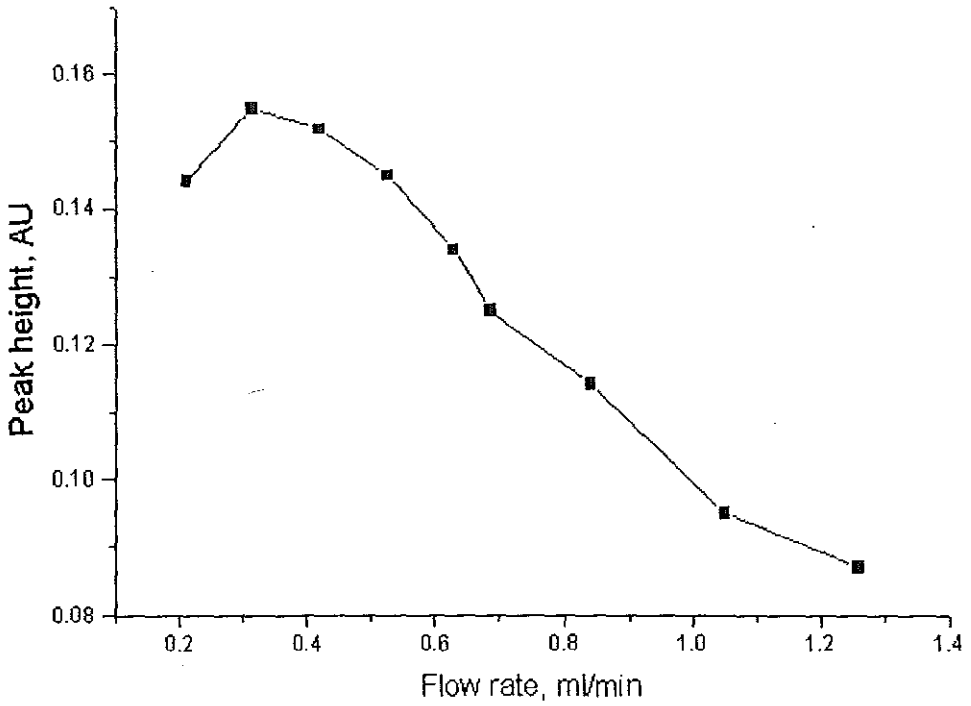

Fig. 4 Effect of total flow rate on the flow injection peak heights for 300 μM ODAP. Injection volume was 20 μl, and carrier /reagent flow rate ratio was 1:0.4.

The effect of GIOD reactor size on the maximum peak height and therefore on the sensitivity and linear range of ODAP determination was studied using reactors of various sizes: 250-μl, 200-μl and 150-μl. A wider linear range was obtained for a 250-μl reactor with sensitivity of 0.41 AU/mM; the linear range was found to be 10 - 300 μM. Better sensitivities for the 150 and 200-μl reactors (0.88 AU/mM and 0.66 AU/mM respectively) were obtained. However, the linear ranges of these reactors were narrow, 10 - 50 μM and 10 - 80 μM respectively. Thus, for the determination of β-ODAP in the isomerization experiments and in grass pea samples the 250-μl reactor was selected because of the wider linear range.

4.2 CALIBRATION OF THE FI SYSTEM

Injections of 20-μl standard produced calibration curves that were linear in the range 10 - 300 μM ODAP. Studies on the linear range of the flow system for the determination of glutamate and hydrogen peroxide showed that the linear range is the

same for both substrates within the studied ranges: 5 - 1000 μM. For the same reactor size (250-μl), the linear range in the present work was narrower than for the reported FI system (10 - 650 μM) [27]. This might be due to differences in geometry and length of the two FI systems. However in the linear region, the conversion efficiency of the reactor for ODAP was 100% and this was an advantage obtained in this work. The increased conversion efficiency was due to higher enzyme activity utilized (80 U/200 mg CPG) during immobilization compared with that used by Moges and Johansson (42 U/150 mg) [27].

The absorbance of 1 mM aspartate corresponds to the value obtained for 150 μM ODAP. This shows that the response of the GIOD reactor in the FI system was more than 6 times for ODAP as compared to aspartate. The reported percentage conversion of aspartate in a 250-μl GIOD reactor relative to glutamate is about 15% [27] but this should depend on the active enzyme loading.

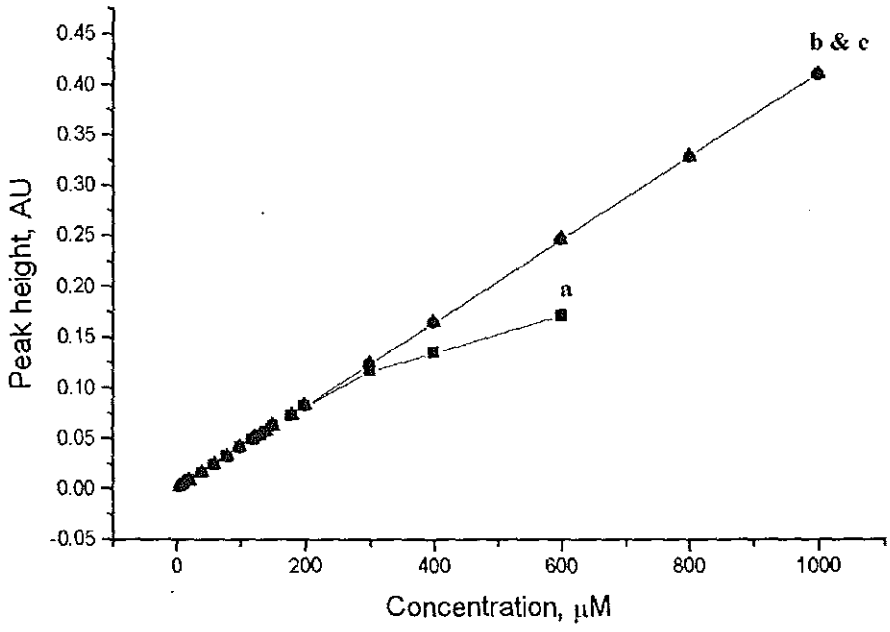

Fig . 5 Calibration curves for ODAP (a), Glutamate (b), and hydrogen peroxide (c).

4.3 ISOMERIZATION KINETICS

4.3.1. The Effect of Concentration

The effect of concentration on the isomerization kinetics was studied by keeping various β-ODAP standards (pH 7) at 80°C for various times. The report by Moges and Johansson [27] has shown that a study on the isomerization of the neurotoxin can conveniently be made with the FI system. The study showed that GIOD is selective to the β form of ODAP.

β-ODAP undergoes a slow transformation to the α-isomer in water at room temperature. The interconversion is facilitated when heated [16, 20]. The reported equilibrium concentrations of the β- and the α- isomers are between 60 - 65% and 40 - 35% [19, 20] respectively. In this work the equilibrium concentrations of the two isomers were studied for various β-ODAP standards and the percentage of the toxin in the equilibrium mixture after incubation was found to be 63% (relative standard deviation 1.3%, n = 5). A recent FI report based on GIOD reactor showed that at equilibrium the two isomers exist as 62% β-ODAP and 38% α-ODAP [27]. Hence, the result obtained in this work is in good agreement with the previously reported values (t-test of 99% probability) which reconfirms the selectivity of the enzyme, GIOD, to the β-isomer [27].

In the kinetic study, initial reading was made one min after β-ODAP was added because the mixing processes affect the rate of isomerization (thus measurement should be taken after steady state is established). During this time interval 10% of β-ODAP was isomerized. Data in Table 1 represent these values. The relationship between the time of equilibration and initial concentration of β-ODAP was found to be linear (Fig. 6). This partly explains the long times required for equilibration (ca. 20 - 48 hr at 55 °C) of very high ODAP concentrations, 3 - 5 mg ODAP in 1 - 1.5 ml D_2O, [19, 20], corresponding to 15 - 28 mM.

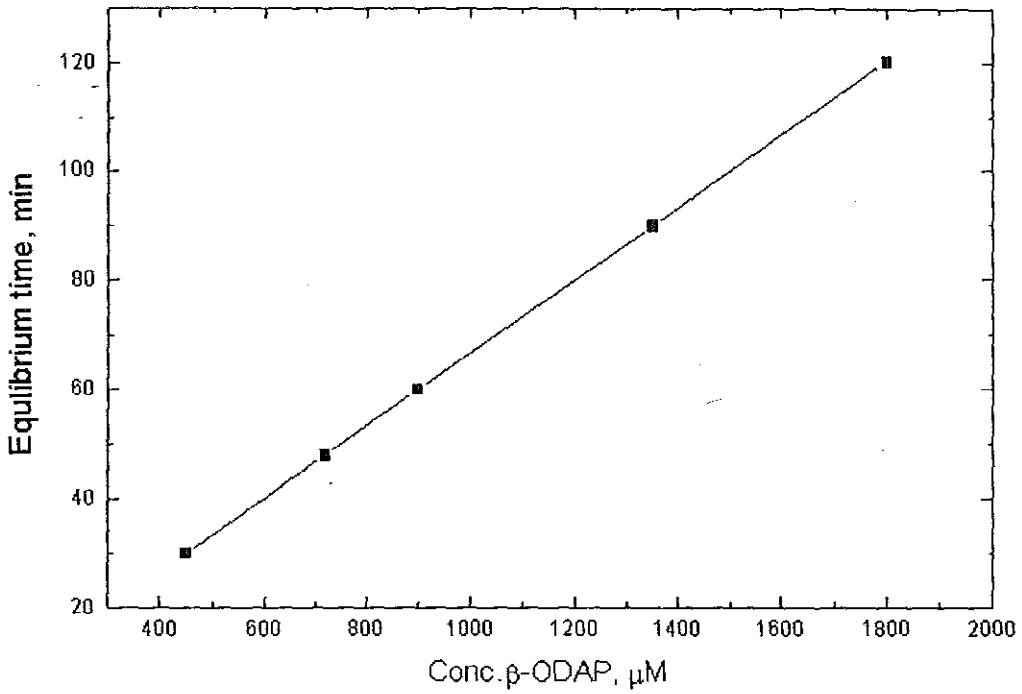

Fig. 6 Plot of initial concentration of β-ODAP vs equilibrium time

To the best of our knowledge no report has been made for the kinetic study of the isomerization process. In this work, an attempt was made to determine the rate constant and order of the isomerization process of the toxic to the non-toxic isomer. The initial apparent rate constant of the $\beta \rightleftarrows \alpha$ conversion, evaluated during the first 10 min, was found to be independent of concentration (Table 1).

Table 1

Initial apparent rate of isomerization*,	15	15.5	15	15.5	15.3
Conc.standard β-ODAP, μM	450	720	900	1350	1800

* average of duplicates

The plot of ln rate against ln [β-ODAP] is a horizontal line of slope zero and intercept ln k_o (Fig.7). This experimental finding suggests that the isomerization

process follows **zero order** kinetics. Furthermore, the linear relationship that exist between equilibrium time and concentration strengthen the suggested zero order kinetics for the isomerization process (see the following mathematical treatment).

From equation 2.6.13 we have,

$$([A] - [A]_o) = -k_{app}t$$

Thus,

$$[A]_\infty - [A]_o = -k_{app}t_\infty$$

or

$$(m[A]_o - [A]_o) = -k_{app}t_\infty$$

where at t_∞, $[A]_\infty = m[A]_o$; the value of m in this particular case is 0.6.

Rearranging the above equation yields,

$$[A]_o (m - 1) = -k_{app}t_\infty$$

Therefore, the time to reach equilibrium is directly proportional to the initial concentration of $[A]_o$.

If the conversion had been first order, the equilibrium time would have been the same irrespective of the initial concentration. This is evident from equations 2.6.4 and 2.6.7.

At t_∞, $[A]_\infty = m[A]_o$, thus equation 2.6.7 takes the form

$$\ln ([A]_o - j)/(m[A]_o - j) = -(k_1 + k_1') t_\infty$$

where $j = k_1' [A]_o/(k_1 + k_1')$

Substituting the value of j into the above equation yields

$$\ln k_1 /(k_1' (m-1) + mk_1) = -(k_1 + k_1') t_\infty$$

From this last equation it is evident that the time needed for equilibration is independent of the initial concentration of A.

The initial apparent rate constant for the conversion of the toxin to the non-toxic isomer was found to be 15.26 μM/min (2.54×10^{-7} M/sec, relative standard deviation 1.64%, n = 5).

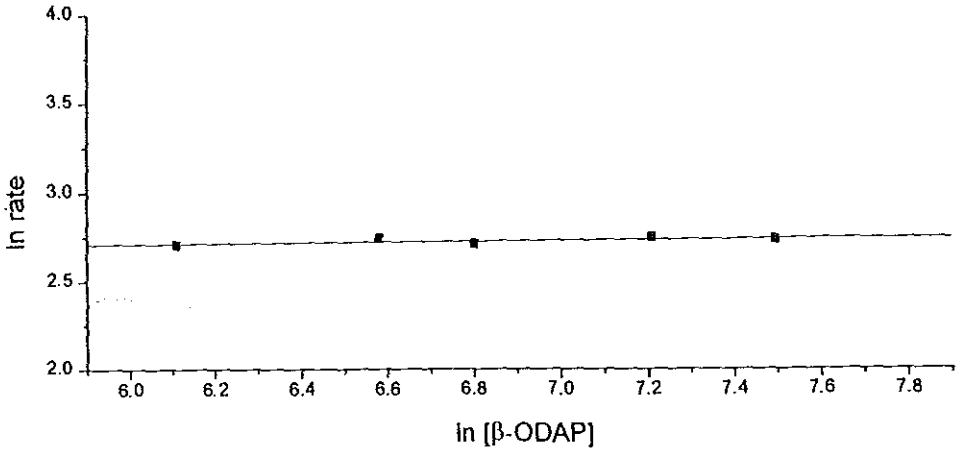

Fig. 7 Plot of ln rate vs ln [β-ODAP]

The fact that the initial apparent rate of isomerization of β-ODAP to α-ODAP is independent of its concentration and does not appear in the rate law suggests a rapid formation of an intermediate. The break down of this intermediate to both isomers in the reverse process is therefore suggested to be the rate limiting step. Accordingly a possible reaction route which may involve during isomerization is suggested as follows:

$$\beta\text{-ODAP} \rightleftarrows \text{I}$$

$$\text{I} \rightleftarrows \alpha\text{-ODAP}$$

Bell and O'Donovan [16] have suggested a cyclic intermediate to be involved during the isomerization process. Later on Abegaz and coworkers [20] have suggested the formation of same cyclic intermediate, via intramolecular rearrangement, because they found that higher homologies of ODAP (structure shown below, n = 3 or 4) do not isomerize as the amine and oxalyl groups are far from each other.

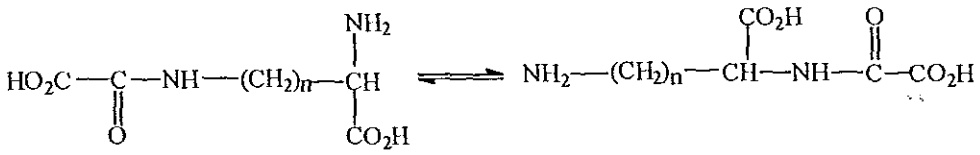

n = 1 β-ODAP
n = 2 γ-ODAB
n = 3 δ-OORN
n = 4 ε-OLYS

n = 1 α-ODAP
n = 2 α-ODAB

4.3.2 The Effect of Temperature

The effect of temperature on the equilibrium time, and the rate of isomerization was studied using 1 mM standard β-ODAP solutions at 60, 70, 80 and 90°C for various times.

When 1 mM standard β-ODAP solution was kept at 60°C, only 71.4% of the toxin was detected at equilibrium which occurred after 3 hr (200 min). The initial apparent rate of isomerization at this temperature was found to be 3.86 μM/min. For the same concentration of standard β-ODAP at 70°C, the initial apparent rate constant of isomerization was 6.8 μM/min. The concentration of the toxin at this temperature was found to be 70% of the initial concentration after 105 min. This concentration did not change even after 165 min showing that equilibrium had already reached. At 80°C, the initial apparent rate constant of isomerization, for 1 mM standard, was 15.26 μM/min. The equilibrium time at this temperature was significantly reduced; only 60 min was needed to reach equilibrium. The initial apparent rate constant of isomerization at 90°C was found to be 30.89 μM/min. The equilibrium time is expected to be about half of that at the lower temperature.

The above experimental findings showed that for an increase in temperature by 10°C there was a corresponding increment in the rate of the isomerization reaction by about two fold. This is in accordance with the Arrhenius relation describing the effect of temperature on the rate of a chemical reaction. Furthermore, for a 10°C rise in temperature, the equilibrium time reduced by about half.

From the initial apparent rate constants at different temperatures, the activation energy, E_a, of the isomerization process was determined using the Arrhenius relation. Plot of ln k_o against the reciprocal of the absolute temperature, 1/T, gives straight line of slope $-E_a/R$ (Fig.8) with intercept ln A, where A is the pre-exponential factor. The corresponding value of the activation energy is 72.2 KJ/mol.

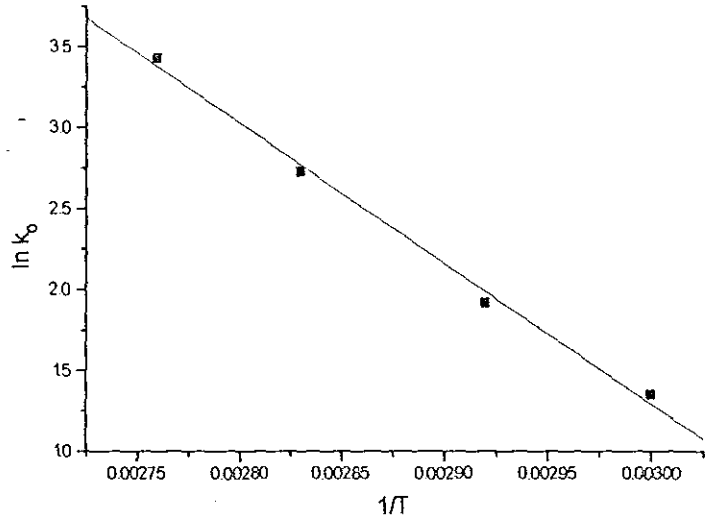

Fig.8 Plot of ln k_o vs 1/T

4.3.3 The EFFECT OF pH

β-ODAP undergoes three acid dissociation steps similar to that of L-glutamic acid. The compound has apparent pK_a values in the order of 1.95, 2.95 and 9.25 corresponding to the two carboxyl and *α*-amino functions, respectively [9, 81]. Thus, like other amino acids, *β*-ODAP takes various forms at different pH values. In this work, 1 mM standard *β*-ODAP (at pH 2) kept in a water bath, thermostated at 80°C, underwent isomerization at an initial apparent rate constant of 24.5 *μM*/min. For this pH value during the first minute it was found that 13% of the toxin was already converted into the *α*-form and equilibrium was attained within 35 min. The equilibrium concentration of the toxin was about 60%. Comparison of values obtained at pH 7 (see section 4.3.1) and pH 2 showed that the isomerization process was faster at pH 2 and the equilibrium time reduced significantly. The possible reason for the increased rate of isomerization, as suggested by Abegaz and coworkers [20], may be the existence of a more preferred rotamer that may dominate at pH 2 than at pH 7. Additionally, the mechanism may involve the reaction of a protonated oxalyl carboxyl group which would be more evident at pH 2 than at pH 7 as the pK_a of this group in *β*-ODAP is 1.95 [9, 81]. The slightly low concentration of *β*-ODAP at equilibrium (60%) is expected to be due to the formation of small amount of DAP, presumably resulting from hydrolysis of the oxalyl compound, which is not

unexpected at pH 2 [20]. Fig. 9 shows concentration of β-ODAP as a function of time for pH 2 and 7.

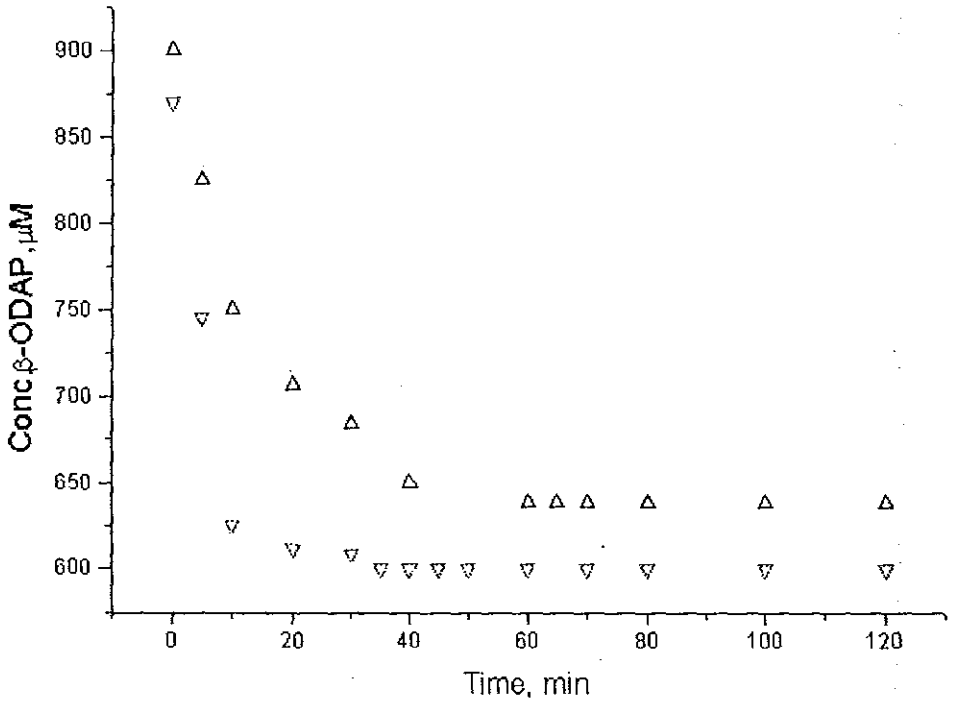

Fig.9 Plots of concentration of the toxin *vs* time during isomerization: ▵ corresponds to pH 7 and ▿ to pH 2

4.4 ATTEMPTS MADE TO OPTIMIZE SIMPLER METHODS FOR PROTEINS SEPARATIONS FROM GRASS PEA EXTRACTS

Moges and Johansson [27] reported that the response of the FI-GIOD reactor for β-ODAP determination became erratic and unreliable after direct injection of a number of crude LS extracts were made into the reactor. This was attributed to the adsorption of proteins and accumulation of cell fragments on the surface of the solid biocatalyst and they used an off-line ultra-filtration step to separate proteins from the extract. Thus, sample pre-treatment before injection becomes apparent to obtain reliable experimental data and to prolong the lifetime of the GIOD reactor. Various methods for the separation of proteins are available [48-50]. The fact that ultra-

filtration membranes are not commonly available urged us to test other options which could be equally useful for this purpose.

The first tested method in this work was solid-phase extraction (SPE). As a model 1 ml of bovine serum albumin (0.3 mg/ml) was allowed to pass through a 1 g ISOLUTE SI (IST, part no. 406-01001 B) column which was previously solvated with 10 ml of hexane and pre-equilibrated with 0.1 M phosphate buffer (pH 7). Absorbance measurement (at 280 nm) of the eluent and the standard revealed that 92% of the protein was retained on the cartridge. Following the same solvation and pre-equilibration procedures, tests were made if ODAP could be eluted without being retained. 1 ml of solution of 200 μM ODAP was allowed to pass through the column but 75% of the compound was retained at the specified pH indicating that isolation of the proteins would not be successful under the given conditions. Studies to optimize the pH at which the amino acid is eluted while the protein is retained is suggested for future work.

Precipitation of proteins directly from grass pea extracts was also made with 5% trichloroacetic acid, TCA. This resulted in a clear solution after centrifugation [48]. Measurement of absorbance at 280 nm showed that more than 70% of proteins were removed from the extract. Injection of the supernatant after pH adjustment (pH 6-7) resulted in very low ODAP concentration (ca. 0.11%). This might be due to the hydrolysis of the toxin to DAP during the TCA precipitation. The pH of the resulting solution was about 0.8.

4.5 DETERMINATION OF β-ODAP IN GRASS PEA SAMPLES

Moges and Johansson [27] reported a selective FI system for the determination of the toxin in grass pea seeds using immobilized GlOD with GlOD and Cat pre-reactors. They demonstrated that any glutamate that would occur in the samples could be completely destroyed. The absence of aspartate in grass pea samples was confirmed by a separate enzymatic procedure. However, they did not compare the analysis results with an independent method.

The complete flow injection set-up, described in Fig. 3, was used to determine the β-ODAP content of five grass pea samples. The GlOD-catalase containing pre-reactor quantitatively destroyed glutamate up to 500 μM but gave an increasing response at higher concentrations. Injections of hydrogen peroxide solutions showed

no response up to the studied limit, 1500 μM. The response of the pre-reactor-containing manifold to 100 μM aspartate was less than 3% of the response to 200 μM ODAP. The previous study showed that only about 5% of the neurotoxin would also be oxidized in pre-reactors containing GIOD and catalase [27].

Direct injections of the extracts resulted in a gradual decrease in responses. This was attributed due to possible adsorption of proteins and accumulation of cell fragments on the surface of the enzyme glass [27]. Attempts to restore the reactors performances by washing with acid buffer (pH 5.7) (as recommended earlier [27]) did not produce significant improvement. Therefore, frequent calibrations of the system between sample injections were necessary.

Determination of the β-ODAP level in five seed samples was made in the presence and absence of the Cat and GIOD containing pre-reactor. The toxin concentration of these grass pea samples was found to be between 0.599 and 0.732% (see Table 2). Removal of the GIOD-catalase containing pre-reactor had essentially the same results (Table 2), indicating that the glutamate content of the seeds was nil or very low. Furthermore, spiking of one of the samples (S-5) with 250 μM glutamate had no effect on the analyses results, demonstrating the absence of interference from this substrate.

The toxin concentrations of the first three samples (S-1, S-2, S-3) were also determined by an independent worker (see Table 2) by measuring absorbances of aqueous extracts at 476 nm following the modified form of the OPT method [80]. Comparison of the means of the FI data with those of the OPT method by the t-test show that the results are not significantly different at more than 95% confidence levels.

Samples S-1, S-2 and S-3 were kept in a thermostated water bath at 80 °C for an hour. Proteins in the extracts were denatured and precipitated. Injections of filtrates of the extracts resulted in absorption peaks which corresponded to 62 - 63 % of the β-ODAP concentration determined before isomerization. Measurements were made in the presence and absence of the pre-reactor. The analyses results in both columns of Table 3 produced additional evidence for the absence of glutamate and other interferences.

Table 2 Determinations of ODAP in grass pea samples in presence and absence of GlOD/Cat pre-reactor. The last column represents results of independent OPT colorimetric method

Sample	Acc. no. (Acc/Sei)	% β-ODAP found using FI system		% ODAP found with OPT method (n = 1)
		In the absence of pre-reactor*	In the presence of pre-reactor*	
S-1	385/504	0.668±0.021	0.670±0.013	0.698
S-2	392/505	0.610±0.022	0.607±0.021	0.630
S-3	462/527	0.743±0.040	0.732±0.030	0.701
S-4	482/530	0.599±0.000	0.597±0.002	
S-5	486/531	0.634±0.048	0.637±0.042	
S-5**	486/531		0.641±0.033	

* 95% confidence limits of triplicate injections.

** Spiked with 250 μM glutamate.

Table 3 Determination of β-ODAP in grass pea samples after isomerization in presence and absence of the GlOD/Cat containing pre-reactor

Sample	% β-ODAP determined after isomerization	
	in the absence of prereactor*	in the presence of prereactor*
S-1	0.412±0.019	0.421±0.010
S-2	0.396±0.020	0.385±0.023
S-3	0.470±0.029	0.462±0.026

* 95 % confidence limits of triplicate injections.

4.6 STABILITY OF THE REACTORS

The sensitivity of the reactor indicated in section 4.1 remained essentially constant for about 4 months when pure samples of β-ODAP were injected. The reactors responses decreased to about 30% after ca.50 injections of grass pea extracts.

The major problem at present is the slight turbidity which arises during extraction. This is expected to be responsible for the deterioration of the reactors performances. Moges and Johansson filtered the extracts by ultrafiltration membranes [27] and this significantly improved the stability of the reactors during the FI runs. In the present study extractions of β-ODAP were also made with buffers containing 500 μM EDTA, and that removed the turbidity. None of these samples were, however, analyzed with the FI system because of the low reactor responses by the time the experiments were being terminated. The results of the EDTA-based extractions suggest that it is not only biological macromolecules that could block and deactivate the enzymes but also metal precipitates which may not dissolve in the carrier-EDTA, immediately after injection.

In view of the problems of reactors stability cited above, it would be appropriate to recommend the following studies before the FI system is adopted for a rapid and selective assay of the toxin in grass pea.

a) Further studies of feasible sample clean-up procedures to separate proteins and other biological macromolecules should be made.
b) Studies of comparison of the effect of grass pea extracts with and without EDTA on the stability of the GIOD reactor in the FI system is recommended.

5.0 CONCLUSIONS

The selectivity of the enzyme GIOD to β-ODAP and the experimental convenience of the FI system to assay small concentrations of the toxin, in μM, were exploited to make rate studies with respect to the effects of concentration of the toxin, temperature, and pH on the conversion of β-ODAP to α-ODAP. Such studies have not been made by other methods. In NMR, for example, quantitative kinetic studies of β-α conversion could not be presented because of the very high concentrations of the toxin used. In this work, an attempt was made to determine the order of the β-α conversion of the neurolathyrogen. Studies on the effect of the concentration of the toxin showed that the isomerization process follows zero order kinetics.

Comparison of the toxin level of *lathyrus sativus* seeds determined by the FI-GIOD based system and the well known OPT method shows that the analysis results are in good agreement.

In the present investigation attempts to separate proteins from *lathyrus sativus* extracts using TCA precipitation and SPE techniques were unsuccessful. Further studies in this regard will have to be made for effective separation of macromolecules and proteins. Provided that stability problems with respect to reactors are solved, the FI-GIOD based method could be applied to rapid and selective determination of β-ODAP in grass pea samples. This would partially answer the question raised by workers in the area of agronomy and genetic engineering for the development of low or non-toxic *lathyrus sativus* seeds.

6.0 REFERENCES

1. D.F. Cohn and M. Streifler, *Arch. Toxicol.*, **191** (1983) 190.
2. S.L.N. Rao, World Review of Nutrition and Dietetics, Vol.**10**, 1969, pp. 214.
3. G. Rosenthal and F. Lambein, eds., Abstract in International Workshop on Ecology and Biochemistry of Non-Protein Amino acids from Plants, Ghent, Belgium, Sept. 17- 19, 1990.
4. D.F. Cohn and M. Streifler, *Archives Suisses de Neurologie, Neurochirurgie et de Psychiatrie*, **128** (1981) 151.
5. R.T. Haimanote, Y.Kidane, E. Wuhib, A. Kalissa, T. Alemu, Z.A. Zein and P.S. Spencer, *Int.J.Epidemiol.*, **19** (1990) 664.
6. T. Gebre-ab, Z. Wolde Gabriel, M. Maffi, Z. Ahmed, T. Ayele, and H. Fanta, *Ethiop. Med. J.*, **16** (1978) 1.
7. B.K. Misra, S.P. Singh, and G.K. Barat, *Qual. Plant Foods Hum. Nut.* **30** (1981) 259.
8. M.V. Barrow, C.F. Simpson and E.J. Miller, *Quart. Rev. Biol.*, **49** (1974) 101.
9. S.L.N. Rao, P.R. Adiga and P.S. Sarma, *Biochem.*, **3** (1964) 432.
10. V.V.S. Murti, T.R. Seshadri and T.A. Venkitasubramanian, *Phytochem.*, **3** (1964) 73.
11. M.Y. Quereshi, D.J. Pilbeam, C.S. Evans, and E.A. Bell, *Phytochem.*, **16** (1977) 477.
12. P.S. Spencer, D.N. Roy, A. Ludloph, J.Hugon, M.P. Dwivedi and H.H. Schaumburg, *Lancent*, **2** (1986) 1066.
13. S. Pearson and P.B. Nunn, *Brian Research*, **206** (1981) 178.
14. R.A. Chase, S. Pearson, P.B. Nunn and P.L. Lantos, *Neuroscience Lett.*, **55** (1985) 89.
15. F. Lambein, G. Ongena and Y.H. Kuo, *Phytochem.*, **29** (1990) 3793.
16. E.A. Bell, and J.P. O'Donovan, *Phytochem.*, **15** (1966) 1211.
17. Y.H. Kou and F. Lambein, eds., Abstract, Lathyrus and Lathyrism, Progress and Prospects, Second International Colloquium on Lathyrism in Bangladesh, Dec.10-12, 1993.
18. S.L.N. Rao, *Anal.Biochem.*, **86** (1978) 386.

19. J.K. Khan, N. Kebede, F, Lambein and A. De Bruyn, *Anal.Biochem.*, **208** (1993) 237.
20. B.M. Abegaz, P.B. Nunn, A. De Bruyn and F. Lambein, *Phytochem.*, **33** (1993) 112.
21. P.O' Brien and P.B. Nunn, *Inorg.Chim.Acta.*, **66** (1982) 185.
22. G.E. Kisby, D.N. Roy and P.S. Spencer, *J.Neurosci.Methods*, **26** (1988) 45.
23. A. Geda, C.J. Briggs and S. Venkataram, *J.Chromatography*, **635** (1993) 338.
24 M.R. Euerby, P.B. Nunn and L.Z. Patridge, *J.Chromatography*, **466** (1989) 407.
25. D.R. Rao, K. Hariharan and K.R. Vijayalakshim, *J.Agr.Food.Chem.* **22** (1974) 1146.
26. G. Moges, T. Solomon and G. Johansson, *Anal.Lett.*, **27** (1994) 2207.
27. G. Moges and G. Johansson, *Anal.Chem.* **66** (1994) 3834.
28. T. Palmer, "Understanding Enzymes", second ed., Ellis Horwood, New York 1985.
29. G.G. Guilbault, "Analytical Uses of Immobilized Enzymes", Chapter 2, Marcel Dekker, New york, 1984.
30. P.W. Carr and L.D. Bowers, "Immobilized Enzymes in Analytical and Clinical Chemistry, Fundamentals and Applications", Wiley, New York, 1980.
31. H. Kuakabe, Y. Miodorikawa, A. Kuninaka, H. Yoshino, *Agric.Biol.Chem.*, **47** (1974) 179.
32. A.M. Klibanov, *Anal.Biochem.*, **93** (1979) 1.
33. K. Mosabch, "Methods in Enzymology", K. Mosbach ed., Academic press, New York, Vol. **XLIV**, 1976
34. F.M. Richards and J.R. Knowels, *J.Mol.Biol.* **37** (1968) 231.
35. H.H. Wettal, "Methods in enzymology", K. Mosbach, ed., Vol. **XLVII** Academic Press, New York, 1976,
36. K. Martinek, A.M. Klibanov, V.S. Goldmacherzin and I.V. *Berezin, Biochim. Biophys.Acta.*, **485** (1977) 1.
37. K. Martinek, N.L. Klyachko, A.V. Kabanov, Y.L. Khmelnitsky and A.V. Levashov, *Biochim. Biophys. Acta.*, **981** (1989) 161.
38. H.H. Wettal, *Anal.chem.*, **46** (1974) 602A.
39. G.G. Guilbault, "Handbook of Enzymic Methods of Analysis", Marcel Dekker, New York, 1976.

40. L.D. Bowers, *Anal.chem.*, **58** (1986) 513A.
41. L.Gorton, E. Csöregi, E. Dominguez, J. Emnèus, G. Jönsson-Petterson, G. Marko-Varga and B. Persson, *Anal.Chim.Acta.*, **250** (1991) 203.
42. L.D. Bowers and P.W. Carr, *Anal.Chem.* **48**, (1976) 544A.
43. E. Reisel and E. Katchalski, *J.Biol.Chem.*, **239** (1964) 1521.
44. R.Q. Thompson and H. Kim, *Biochim.Biophys.Acta.*, **964** (1988) 116.
45. W.E Morf, Mikrochim.Acta., **2** (1980) 317.
46. G. Johansson, L. Ögren and B. Olsson, *Anal.Chim.Acta.*, **145** (1983) 71.
47. B. Olsson and L. Ögren, *Anal.Chim.Acta.*, **145** (1983) 87.
48. D.M. Bollag and S.J. Edelstein, "Protein Methods", Third ed., Wiley-Lis, New York, 1992.
49. H. Lingeman and U.R. Tjaden, "Detection-Oriented derivatization techniques in liqud chromatography", Marcel-DeKker Inc., New York, Ch.3, 1990.
50. R.K. Scopes, "Protein Purification, Principles and Practice" Third ed., Springer-verlag, New York, 1994.
51. R. D. McDowell, *J.Chromatography*, **492** (1989) 3.
52. G. Nagy, Z. Feher, and E. Punger, *Anal.Chim.Acta.*, **52** (1970) 47.
53. J. Ruzicka and E.H. Hansen, *Anal.Chim.Acta.*, **78** (1975) 145.
54. K.K. Stewart, G.R. Beecher, and P.E. Hare, *Anal.Biochem.*, **70** (1976) 167.
55. J. Ruzicka and E.H. Hansen, "Flow Injection Analysis", First ed., Wiley, New York, 1981.
56. J. Ruzicka and E.H. Hansen, *Anal.Chim.Acta.*, **99** (1978) 37.
57. J. Ruzicka and E.H. Hansen, *Anal.Chim.Acta.*, **92** (1977) 235.
58. A.U Ramsing, J. Ruzicka and E.H. Hansen, *Anal.Chim.Acta*, **129** (1981) 1.
59. R. Tijssen, *Anal.Chim.Acta.*, **114** (1980) 71.
60. K. Kronkvist, K. Wallentin and G. Johansson, *Anal.Chim.Acta.*, **290** (1994) 335.
61. M. Massom and A. Townshed, *Anal.Chim.Acta.*, **171** (1985) 185.
62. M. Massom, *Anal.Chim.Acta.*, **214** (1988) 175.
63. T. Yao and T. wasa, *Electroanalysis*, **5** (1993) 887.
64. G. Moges and G. Johansson, *Anal.Lett.*, **27** (1994) 495.
65. G. Moges, Ph.D. Thesis, Addis Ababa University, 1994.
66. X. Yang, *Biosensors*, **4** (1989) 131.

67. M. Skoog, G. Johansson B. Olsson and R. Appelquvist, *Microchim.Acta*, **3** (1988) 131.

68. L.C. Clark Jr., "Methods in Enzymology", Vol. **56**, Academic Press, New york, 1979, pp. 448.

69. T.E. Barman, "Enzyme Handbook", Vol. 1, Springer Verlag, New york, 1969.

70. D. Barham and P. Trinder, *Analyst*, **97** (1972) 142.

71. B. Olsson, *Mikrochim.Acta*, **2** (1985) 211.

72. H.B Dunford and J.S. stillman, *Coord.Chem.Rev.*, **19** (1976) 81.

73. M.A. DeLuca, ed, "Methods in Enzymology", Vol. **LVII**, Academic Press, New york, 1978.

74. J.W. Hall and D.M. Tucker, *Anal.Biochem.*, **26** (1968) 12.

75. P. Trinder, *Ann.Clin.Biochem.*, **6** (1969) 24.

76. F. Wilkinson, "Chemical Kinetics and Reaction Mechanism", Van Norstrand Reiuhold limitted, New York, 1980, Ch. 3, pp.50.

77. S.M Smith, "Chemical Engineering Kinetics", McGraw-Hill, Tokyo, 1981, Ch.2, pp. 62.

78. J.L. Latham and A.E. Burgess, "Elementary Reaction Kinetics", Third ed., Bulterworths, Sydeny, 1980.

79. G.T. Hermanonson, A.K. Mallia and P.K. Smith, "Immobilized Affinity Ligands Techniques", Toronto, 1992, pp. 287.

80. R.T. Haimanote, B.M. Abegaz, E. Wuhib, A. Kassina, Y. Kidane, N. Kebede, T. Alemu and P.S. Spencer, *Nutrition Research*, **13** (1993) 1113.

81. P.O' Brien and P.B. Nunn, *Phytochem.*, **21** (1982) 2001.

DECLARATION

I, the undersigned, declare that the thesis is my original work and has not been presented for a degree in any other University.

Name: Abebaw Belay

Signature: 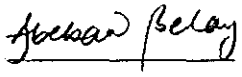

Date of Submission: June, 1995

This thesis has been submitted for examination with our approval as University advisors.

Dr Ghirma Moges 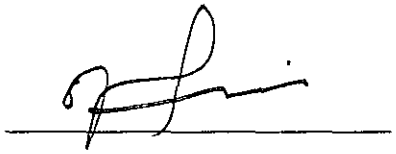

Dr Theodros Solomon